## General Disclaimer

## One or more of the Following Statements may affect this Document

- This document has been reproduced from the best copy furnished by the organizational source. It is being released in the interest of making available as much information as possible.

- This document may contain data, which exceeds the sheet parameters. It was furnished in this condition by the organizational source and is the best copy available.

- This document may contain tone-on-tone or color graphs, charts and/or pictures, which have been reproduced in black and white.

- This document is paginated as submitted by the original source.

- Portions of this document are not fully legible due to the historical nature of some of the material. However, it is the best reproduction available from the original submission.

DRA

NASA

Technical Memorandum 83975

# Accretion Powered X-Ray Pulsars



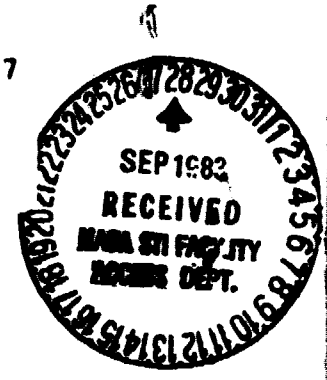


N. E. White, J. H. Swank and S. S. Holt


AUGUST 1982

National Aeronautics and
Space Administration

**Goddard Space Flight Center**
Greenbelt, Maryland 20771

# ACCRETION POWERED X-RAY PULSARS

N.E. White[1], J.H. Swank, and S.S. Holt
Laboratory for High Energy Astrophysics
NASA/Goddard Space Flight Center
Greenbelt, Maryland 20771

## ABSTRACT

A unified description of the properties of 14 X-ray pulsars is presented and compared with the current theoretical understanding of these systems. The sample extends over six orders of magnitude in luminosity, with the only trend in the phase averaged spectra being that the lower luminosity systems appear to have less abrupt high energy cutoffs. There is no correlation of luminosity with power law index, high energy cutoff energy or iron line EW. Detailed pulse phase spectroscopy is given for five systems. The $180^{o}$ phase reversals from one energy band to the next seen from the $L_X > 10^{37}$ erg $s^{-1}$ systems 4U1626-67 and GX1+4 can be interpreted as being caused by the emission switching from a fan to a pencil beam configuration, as discussed by Nagel (1981a) for a cylinder of emission. We point out that if there is a collisionless shock in the $L_X < 10^{37}$ erg $s^{-1}$ systems then the observed properties of these systems might be expected to resemble those with higher $L_X$ where there should be a radiative shock. The pulse profiles of the lower $L_X$ systems do not show $180^{o}$ phase reversals and are in qualitative agreement with the predictions of the thin slab models.

The pulse phase spectra of 4U0115+63 first reported in Rose et al. (1979) are re-examined and it is shown that there are electron cyclotron lines at

11.5 and 23 keV that appear to be in absorption at the pulse peak and in emission during an interpulse. Regions of spectral hardening or "notches", similar to that reported by Pravdo et al. (1977b) from Her X-1, are a common feature in the low energy pulse of many pulsars. These probably represent the passage of the magnetic axis through our line of sight. The material flowing through the magnetosphere does not appear to contribute to the pulse beaming We discuss the nature of the beaming from Her X-1 in the context of these new results and conclude that a pencil beam configuration most simply explains the overall properties of the pulse. It is suggested that by analogy with 4U0115+63 that the feature in the spectrum of Her X-1 is an absorption line at ~ 35 keV and that in the off pulse spectrum this may become an emission feature.

The binary parameters and low X-ray luminosities of X Per, 4U1145-61 and 4U1258-61 suggest that the neutron stars are undergoing spherical accretion. We show that the pulse profiles are much less structured than those of the more luminous pulsars and are qualitatively in agreement with the models of Arons and Lea and Elsner and Lamb.

[1]Also Dept. Physics & Astronomy, University of Maryland

# I. INTRODUCTION

More than a decade has passed since the discovery of the first binary X-ray pulsars Cen X-3 and Her X-1 (Giacconi et al. 1971; Tananbaum et al. 1972). Since then ~ 20 X-ray pulsars have been found with periods ranging from 69 ms to 835s (e.g. Ives, Sanford and Bell-Burnell 1975; Rosenberg et al. 1975; McClintock et al. 1976, 1977; Lucke et al. 1976; White et al. 1976a,b, 1978; Davison 1977; Rappaport et al. 1977; White and Pravdo 1979; Kelley et al. 1981,1982; Skinner et al. 1982). These represent ~ 15% of the known galactic X-ray sources with $L_X \gtrsim 10^{33}$ erg $s^{-1}$. The coherence of the pulsations, and the secular decrease in their periods on timescales of $10^2$ - $10^5$ yrs, established beyond doubt that each of these systems contains a magnetized rotating neutron star accreting material and gaining angular momentum from a binary companion (Lamb, Pethick and Pines 1973; Davidson and Ostriker 1973; Rappaport and Joss 1977; Mason 1977). Measurements of the orbital elements of six systems require that the mass of the pulsar be consistent with that expected for a neutron star (Rappaport and Joss 1982).

Because sharp features in the light curves from many of the pulsars cannot be reproduced from viewing the rotation of an isotropically emitting hot spot, the X-ray emission must be beamed (Basko and Sunyaev 1976b). Such beaming, cyclotron features in the spectra, and magnetic flux conservation at the time of a neutron star's creation all suggest $\gtrsim 10^{12}$ G fields at their surfaces. Only recently have the calculations of the radiative transfer in such superstrong magnetic fields reached a point where they can be meaningfully tested against the observations (e.g. Kanno 1980; Nagel 1981a,b; Pravdo and Bussard 1981; Langer and Rappaport 1982; Meszaros et al. 1982). One key problem that is still unresolved is how the infalling material is stopped. For systems close to the Eddington limit a radiative shock seems

inevitable (Basko and Sunyaev 1976a), but for many X-ray pulsars with lower luminosities it is not clear whether plasma instabilities cause a standoff collisionless shock above the surface, or whether the material is decelerated deeper in the neutron star atmosphere (Basko and Sunyaev 1975; Shapiro and Salpeter 1975; Kirk and Galloway 1981). This issue is crucial to discussions concerning whether the X-rays are beamed along or perpendicular to the field lines, i.e. in a "pencil" or a "fan" beam (e.g. Nagel 1981a). A further complication that remains unresolved is the role played by material in the magnetosphere in determining the pulse profile and spectrum, particularly below a few keV where photoelectric and possibly cyclotron absorption are important (McCray and Lamb 1976; Elsner and Lamb 1976; Basko and Sunyaev 1976b).

An important influence on potential models has been the discovery of a cyclotron feature in the spectrum of Her X-1 at ~ 60 keV (Trumper et al. 1978). Because a detailed measure of the continuum above the feature is below the threshold of current instrumentation, there is considerable controversy as to whether this is an absorption line at ~ 35 keV or an emission line at ~ 60 keV (e.g. Yahel 1979; Bonazzola, Heyvaerts, and Puget 1979; Bussard 1980; Wang and Frank 1981; Langer, McCray and Baan 1980). Pulse profiles have so far provided little to constrain the models in general, since they exhibit remarkable variety, including simple sinusoidal-like variations (e.g. White et al. 1980), complex energy dependent features (e.g. McClintock et al. 1976) and $180^{o}$ phase reversals from one energy band to another (e.g. Rappaport et al. 1977). Wang and Welter (1981) have pointed out that the light curves of the higher luminosity systems are more complex and that this may reflect a basic change in the beaming pattern.

The phase-averaged spectra most often exhibit flat ($\alpha \sim 0$) power laws

with a sharp high energy cutoff at ~ 20 keV (Her X-1, Holt et al. 1974; 4U0900-40, Becker et al. 1978); with others being characterized by slightly steeper power laws ($\alpha \sim 0.4$) with less obvious high energy cutoffs (4U1145-61, White et al. 1980; OA01653-40, White and Pravdo 1979). The low luminosity ~ $10^{34}$ erg $s^{-1}$ pulsar X Per is an exception, being best fit by a ~ 12 keV thermal spectrum in the 2-20 keV band with a power law tail ($\alpha \sim 1.2$) above ~ 20 keV (White et al. 1982; Worrall et al. 1981; Becker et al. 1979). Detailed analysis of the spectral properties across the pulse of Her X-1 show that there is a region of spectral hardening near pulse maximum (Pravdo et al. 1977b,1978). Similar regions of pulse hardening are evident in 4U0115+63 (Johnson et al. 1978; Rose et al. 1979), GX1+4 (Doty, Hoffman and Lewin 1981) and X Per (White et al. 1982). Some attempts have been made to interpret such spectral effects in individual sources (e.g. Pravdo et al. 1977b,1978), but in general these features have not been utilized as crucial factors in determining the validity of models. Iron K shell emission with EWs of several hundred eV has been seen from all these systems except X Per, and may be caused by fluorescence of relatively cool material in the neutron star magnetosphere (Pravdo et al. 1977a; Basko 1980).

The purpose of this paper is to present a unified description of the observed properties of X-ray pulsars in an effort to better constrain the more detailed theoretical models that are currently under development. We increase to 14 the sample of X-ray pulsars for which high quality non-dispersive spectral observations have been reported. These range over six orders of magnitude in X-ray luminosity, and in §II the pulse profiles and phase averaged properties are examined for any systematic trends. Spectral variations with pulse phase are addressed in detail in §III. In §IV we

examine the observed properties of these pulsars for clues as to the direction of the beaming. In §V the nature of the cyclotron features observed in Her X-1 and 4U0115+63 are discussed. The interaction of the inflowing material with the magnetosphere and its subsequent effect on the pulse profile is considered in §VI. Possible origins for the iron line emission seen from most of these systems are discussed in §VII. The current observational picture deduced from these results is summarized in §VIII.

## II. LUMINOSITY CORRELATIONS

### A. The Pulse Profiles

Table 1 lists the names and parameters of the 14 pulsars in our sample. In Figure 1 the pulse profiles of 12 of the pulsars are shown in order of increasing luminosity (from bottom left to top right). The pulse period in seconds and the log of the unabsorbed 0.5 to 60 keV luminosity $L_X$, excluding any soft components, are indicated. We use this particular energy range because 0.5 keV is the lower threshold of the Einstein Solid State Spectrometer (SSS) and 60 keV is the maximum energy seen by HEAO-1 A2. The profile of LMC X-4 is not shown since the 13.5s pulsations are only seen during ~ 20 min flares, but not from the quiescent emission (Kelley et al. 1982). No such flares were seen by any of our detectors; the steady flux seen by HEAO-1 A2 during a 3 hr pointed observation was not modulated greater than 5% peak to mean amplitude, compared to 20% seen by SAS-3 during outburst. For 4U0115+63 a broad band 2-60 keV profile is shown in Figure 10, and is discussed further in §IIIC. There has been some suggestion that the period of GX1+4 is twice that given in Table 1 (Koo and Haymes 1980; Strickman, Johnson and Kurfess 1980), but we find no evidence for this in our data, in particular a power spectrum shows no power at half the frequency of the period given in Table 1 or at any of its odd harmonics; we will assume the shorter period.

As noted by Wang and Welter (1981) there seems to be a trend in the pulse profiles with luminosity despite the variety of high luminosity types which seemed counter to a trend in a smaller sample (Rappaport and Joss 1977a). Below ~ $10^{36}$ erg $s^{-1}$ they are sinusoidal-like with little dramatic dependance on energy, although 4U1145-61 and 4U1258-61 do show a slight decrease in amplitude with increasing energy (as first noted for the latter by McClintock et al. 1977). Between $10^{36}$ and $10^{37}$ erg $s^{-1}$ the profiles become more energy dependent; at high energies the modulations are still simple sine waves but at lower energies the amplitude decreases with the appearance of more complicated structure in some. Such is the case for the recurrent transient A0535+30 (Bradt et al. 1976) which, because we had no data in outburst, is not included. At luminosities above $10^{37}$ erg $s^{-1}$ some of the profiles show $180^{o}$ phase reversals from one energy band to the next (e.g. 4U1626-67). Others have sharp pulses that do not change phase with energy. There is a tendency for the longest pulse period pulsars to have the lowest luminosities, although GX1+4 and OA01653-40 are exceptions to this rule. Another curiosity is that the double peaked light curves tend to occur in the $10^{36}$-$10^{37}$ erg $s^{-1}$ luminosity band. This may be coincidental, but also could reflect a fundamental property of the accretion process or X-ray beaming.

B. Phase Averaged Spectra

The spectra of X-ray pulsars are usually represented by a power law with energy index $\alpha$, modified at energies above a high energy cutoff $E_c$ by the function $\exp[(E_c-E)/E_F]$. Typically this parameterization gives an adequate representation of the high energy portion of the spectrum. In addition, an iron K feature between 6 and 7 keV and a small amount of low energy absorption by cool material are usually required to give an acceptable $\chi^2$. Previous examples of this fitting procedure can be found in Pravdo et al. (1977a,b,

1978, 1979); Swank et al. (1976); Becker et al. (1976, 1977a,b, 1978, 1979); Rose et al. (1979); White and Pravdo (1979) and White et al. (1980). These earlier results, along with those from the new observations, are summarized in Table 1 in the phase-averaged parameters $L_X$, $\alpha$, $E_C$, $E_F$, and equivalent width EW of the iron line. The data utilized come from the GSFC proportional counters on either the HEAO-1 or the OSO-8 observatories and cover the energy range 2-60 keV with 64 channels of PHA for each detector (see the above papers for further details). The deduced incident spectra are shown in Figure 2 in order of increasing luminosity, with the log $L_X$ given at the top right of each spectrum. The de-convolved spectra are not completely independent of the assumed model and will vary slightly for different models that can also give acceptable fits (cf. Holt and McCray 1982). In particular, the representations of narrow features such as lines are sensitive to how they are modelled. The emission features at ~ 6.5 keV can usually be described within the uncertainties by a single narrow line, by a Gaussian with FWHM up to ~ 1 keV or by a multiplet of narrow lines. Figure 2 shows the results for single Gaussian best fits (FWHM ~ 0.4 keV for 4U1538-58 and ~ 1 keV for OA01653-40, for examples.)

Two of the lower luminosity pulsars X Per and 4U1258-61 deviate from the above formalism. The spectral properties of X Per have been discussed in depth by White et al. (1982), Worrall et al. (1981) and Becker et al. (1979). The spectrum in the 1-20 keV band is a simple exponential model with an e-fo'ding energy of ~ 10 keV, but at energies above 20 keV there is a power law excess with $\alpha$ ~ 1.2. Two observations of 4U1258-61 were made by HEAO-1 A2 in January and June 1978. The average source luminosity was ~ 50% lower on the second occasion. The two spectra were similar, a rather steep power law with $\alpha$ ~ 1.2, modified at low energies by ~ $10^{22}$ H $cm^{-2}$ of absorbing

material. No high energy cutoff was required; however high energy observations by Maurer et al. (1982) suggest that there is a sharp high energy break at ~ 20 keV and there may be a hint of this in Figure 2. An observation by the Einstein (SSS) in January 1979 measured a column density of (1.3±0.4) x $10^{22}$ H $cm^{-2}$ and $\alpha \sim 0.3 \pm 0.3$. This source is behind the Coalsack Nebula and the reddening measured by Parkes, Murdin and Mason (1980) is consistent with all the observed X-ray absorption being interstellar in origin. The lower power law index seen by the SSS may indicate a continuum intrinsically flatter below ~ 3 keV, rather than spectral variation.

Two spectra given in Table 1 have been omitted from Figure 2. LMC X-4 is not shown because contributions of a nearby supernova remnant must be taken into account in interpreting the below 4 keV data. The spectrum of 4U1626-67 is not given because it shows radical departures from the mean spectrum as a function of pulse phase; instead spectra from two different pulse phases are shown in Figure 6.

In Figure 3 we show the variation in $\alpha$, $E_C$, $E_F$ and EW with log $L_X$. The dashed lines in Figure 3 indicate the variations in these parameters with pulse phase (taken from Pravdo et al 1979, Rose et al. 1979, and §III below). Except for X Per and 4U1258-61 the range of variation in $\alpha$ from source to source is comparable to the range for a single source over all pulse phases. The cutoff energy $E_C$ is between 10 and 20 keV, with no obvious correlation with luminosity. The form of the spectrum above the cutoff is imposed a priori, and the efficiency of the detectors declines above 20 keV so that lower flux sources have more ill-defined values of $E_f$. Nonetheless with the exception of the two $\gtrsim 10^{38}$ erg $s^{-1}$ sources GX1+4 and LMC X-4 the value of $E_F$ tends to increase with decreasing $L_X$ from ~ 7 keV at ~ $10^{38}$ erg $s^{-1}$ to ~ 25 keV at $10^{35}$ erg $s^{-1}$. In White and Pravdo (1979) and White et al. (1980) we

reported that OA01653-40 and 4U1145-61 did not have detectable high energy cutoffs below 60 keV. Re-analysis of these data with improved background subtraction does reveal a slight attenuation above ~ 20 keV in both sources. The spectrum of GX1+4 is very different from the rest in the sense that the break at 10 keV is barely perceptable because the high energy cutoff is so gradual and it does not fit into the general trend of decreasing $E_f$ with increasing $L_X$.

## III. PULSE PHASE SPECTROSCOPY

The energy dependent variations in the pulse profiles shown in Figure 1 reflect changes across the pulse in the underlying spectrum. Pravdo et al. (1977b, 1978) developed the technique of pulse phase spectroscopy and discuss in detail the spectral properties of Her X-1 as a function of pulse phase. These studies show that its spectrum above 2 keV is constant across the pulse except for a region of hardening that occurs in the vicinity of the "notch" seen just after pulse maximum. Here we examine the pulse phase spectral properties of five more systems.

### A. GX1+4 and 4U1626-67

The luminosity of GX1+4 is ~ $10^{38}$ erg $s^{-1}$, i.e. it is close to the Eddington limit for spherical accretion onto a neutron star. Figure 4 shows the light curve above 25 keV to be roughly sinusoidal. Below 7 keV the maximum shifts by almost $180^{o}$. There is a very distinctive "notch" (first reported by Doty, Hoffman and Lewin 1981) centered on what appears would otherwise be the low energy maximum. This $180^{o}$ phase reversal is reminiscent of a similar phenomenon found in the light curve of 4U1626-67 by Rappaport et al. (1977) and it is useful to compare and contrast the properties of the two. The HEAO-1 A2 light curve of 4U1626-67 is shown in Figure 5 (taken from Pravdo et al. 1979). In this case there are two $180^{o}$ phase reversals and the

3-14 keV band again displays a distinctive "notch" centered on pulse maximum.

In Figure 6 the spectra from the phases centered on the low and high energy maxima are given for both sources. These spectra, smoothed for clarification, are based on the combination of Einstein SSS and HEAO-1 A2 observations. The HEAO-1 A2 incident spectra for 4U1626-67 can be found in Pravdo et al. (1979). The "hard" and "soft" pulse spectra of both 4U1626-67 and GX1+4 cross over at ~ 10 keV and those of 4U1626-67 cross over again at ~ 2.5 keV; such a second crossover in the case of GX1+4 may be masked by an $N_H$ of ~ $10^{22}$ H $cm^{-2}$. The principal spectral parameters of interest are given for each source as a function of pulse phase in Figures 4 and 5, with the latter again taken from Pravdo et al. (1979). The high energy cutoff of GX1+4 is so gradual that the interaction of the various model parameters prevent a unique fit; we chose to fix $E_C$ at the phase-average value for GX1+4 of 10 keV to allow a restricted fitting of $E_F$. In doing so there is a significant increase in $E_F$ at the maximum of the hard pulse at $\phi \sim 0.35$ and an increase in $\alpha$ during the soft pulse (except during the "notch"). The spectral index of 4U1626-67 increases during the hard pulse minimum, with an accompaning reduction in $E_F$. No variation is seen during the 3-14 keV notch at $\phi \sim 0.75$, but finer phase resolution is not possible given the statistical precision of the data. We note that Pravdo et al. (1979) also included a constant luminosity ~ 0.25 keV blackbody component to obtain an acceptable $\chi^2$. The SSS spectra did not require this component, so that its inclusion in the HEAO-1 A2 fits is probably artificial, reflecting the inadequacy of the simple model used (see the discussion in Pravdo et al. 1979).

B. 4U0900-40

The luminosity of 4U0900-40 is $\sim 10^{36}$ erg $s^{-1}$. This pulsar exhibits a pronounced energy dependence in its light curve that is quite different from that of GX1+4 and 4U1626-67. Figure 7 shows that the light curves seen with HEAO-1 A2 during three ~ 6 hr observations appear to be basically the same as that first reported by McClintock et al. (1976), with a double sinusoidal-like modulation at energies > 10 keV that fragments into more detailed structure at lower energies. There are subtle changes in the light curve from one observation to another. Comparing 1977 days 512 and 716 to day 699, for example, reveals that in the latter the minimum D1 at $\phi \sim 0.25$ is much more pronounced and is even observable in the 7-25 keV band; other more subtle differences are apparent in the 2-7 keV band. Such variations may be a function of the luminosity of the source (the average count rate is given in the top right hand corner of each plot). There were many more pointed HEAO-1 A2 observations of 4U0900-40, but only these three could be used for comparison because the source undergoes large variations in absorption (up to $\sim 10^{23}$ H $cm^{-2}$, Becker et al. 1980 and refs therein) and during the other observations the low energy visibility was seriously degraded. In the three cases considered here the absorption was low at $\sim 10^{22}$ H $cm^{-2}$, and while some of the subtle changes in the 2-7 keV band could conceivably be attributed to undetected absorption variations, the changes seen in the 7-25 keV band must be intrinsic to the pulsar itself.

The variation in the spectral parameters as a function of pulse phase are given in Figure 8 for day 699 when the source was bright; there was no significant change in these parameters when the source was fainter. $E_c$ and $E_F$ are relatively constant across the pulse at ~ 20 keV and 10 keV respectively, except for some excursions in $E_F$ on the trailing edge of the two pulses which

may be caused by uncertainties in the background subtraction. The average value of $E_c$ agrees well with the value given by Becker et al. (1978), but is less than the 27 keV found by Staubert et al. (1980) from harder X-ray measurements. In Figure 9 (upper panel) the incident spectra at pulse minimum (L) and maximum (P) are shown and can be seen to be similar in form. The incident spectra during D1 and D2 are given in Figure 9 (lower panel) along with that at maximum (P), with the latter renormalized upwards by 15% to give similar intensities above 20 keV. $\alpha$ does not vary from the minimum (L) to the maximum (P) of the pulse in the 2-7 keV band, but during the features D1 and D2 $\alpha$ changes from 0.5 to -0.25. The spectral hardening during D1 and D2 is attributed to a flattening of the spectrum below 10-20 keV only, with the spectral shape at higher energies apparently unchanged. D1 and D2 do not show the edges and low energy turnover expected from absorption due to a totally obscuring medium and we can rule out the suggestion of Wang and Welter (1981) that this structure is caused by photoelectric absorption due to partially ionized material in the magnetosphere.

C. 4U0115+63

Wheaton et al. (1980), using the hard X-ray (10-100 keV) HEAO-1 A4 experiment, reported evidence for an absorption feature at ~ 20 keV in the pulsed spectrum of 4U0115+63 ($L_X \sim 10^{37}$ erg $s^{-1}$). Rose et al. (1979), using data taken simultaneously with the HEAO-1 A2 detectors (2-60 keV) questioned the significance of this result because they found that the off pulse spectrum itself was structured and they pointed out that this might cause physically meaningless features in the on minus off pulse spectrum (see also Pravdo et al. 1979). The pulse profile of 4U0115+63 (Figure 10) is composed of three distinct features, a sharp peak (P), followed by a broad interpulse (I), ending in a well defined minimum (L). The variations in the spectral

parameters as a function of pulse phase were discussed in Rose et al. (1979) who found a region of spectral hardening during the pulse peak P and possibly also during the interpulse I (see also Johnston et al. 1978). The minimum L was well fit with the standard model, but during the pulse peak and the interpulse the fits to the standard power law plus high energy cutoff model were unacceptable with $\chi^2$ of respectively 50 and 71 for 30 dof. The three incident spectra for each of these phase intervals are also given in Figure 10. This suggests that the poor fits are caused by the appearance of line features at ~ 11.5 and 23 keV, first in absorption during P and then in emission during I; these lines are not related to the iron feature at ~ 6.7 keV. The lines are not evident in the spectrum L. This effect can also be seen in Figure 11 where the ratio of the spectrum during P and I to that at L is shown. The deficiencies and excesses at ~ 11.5 and 23 keV are clearly evident. This effect is amplified by taking the ratio of I/P (Figure 11).

Formal fits to the HEAO-1 A2 data that include an emission line in spectrum I give a line energy of 11.75±0.75 keV with an EW of 3.0±1.5 keV and a FWHM < 5 keV. An absorption line in the P spectrum gives an energy of 11.3±0.9 keV with an EW of 1.5±1.1 keV and a FWHM of < 5 keV. The value of the underlying exponential cutoff also increased from 6 to 12 keV during the spectrum I. The $\chi^2$ were 35 and 45 for 27 dof for the P and I spectra respectively. Including an additional line at 23 keV did slightly improve the $\chi^2$ but because of the relatively poor statistics at high energies and the interaction of the various parameters in the multi-parameter fits, it is not formally required. All the uncertainties are 90% confidence with an additional 5% systematic uncertainty in the estimates of the line energies. These and other various line parameters are summarized in Table 2.

The phase of the HEAO-1 A2 pulse peak agrees well with that given by the ephemeris in Wheaton et al. for their lowest energy band of 13.8 to 16.6 keV. This is contrary to the statement made in Wheaton et al. of a 0.35 phase shift relative to the pulse seen by HEAO-1 A3 at energies similar to our measurement. Above 20 keV the centroid of the pulse seen by Wheaton et al. seems to shift by ~ 0.1 to an earlier phase and there is an associated increase in the duration of the main pulse from ~ 0.2 to ~ 0.5 in phase. By taking on minus off pulse spectra from HEAO-1 A2 we obtained two deep absorption lines at ~ 11.5 and 23 keV. Within the uncertainties of the energy calibration of the A-2 and A-4 instruments, the line that we see at 23 keV is probably consistent with that seen at ~ 20 keV by Wheaton et al. (1979). It is appealling to interpret these features as the 1st and 2nd harmonia of electron cyclotron lines (cf. Wheaton et al. 1979). The energy of ~ 11.5 keV for the fundamental gives the magnetic field at the surface of the neutron star to be ~ $1.2 \times 10^{12}$ G.

D. Cen X-3

The pulse profile of Cen X-3 is qualitatively similar to that of 4U0115+63, a similarity that is made more striking by the fact that they both have the lowest phase averaged high energy cutoffs at ~ 10 keV (cf Table 1 and Figure 1). In Figure 12 the pulse light curve is shown as seen by OSO-8 in four different energy bands. Like 4U0115+63 it consists of a sharp maximum, followed by a broad interpulse ending in a minimum. There are subtle changes in the envelope with energy. The width of the primary peak (P) decreases and then increases from low to high energies, and the interpulse disappears at high energies. The spectral parameters $\alpha$, $E_C$, $E_F$ and the EW of the iron line as a function of pulse phase are shown in Figure 12 when the average luminosity was $0.8 \times 10^{38}$ erg $s^{-1}$. The amplitude of the variations in these

parameters with pulse phase are much less than those discussed earlier. There is a tendency for $\alpha$ to decrease during the pulse peak and the interpulse. The high energy turnover increases during the decay of the primary pulse and at pulse minimum. A second observation of Cen X-3, when $L_x \sim 1.2 \times 10^{38}$ erg $s^{-1}$, exhibited similar parameters, except for an overall decrease in the average value of $E_c$ from 11 to 8 keV. The number of iron line photons across the pulse is approximately constant, and causes a factor 3 variation in the EW. In Figure 13 the incident spectra from three pulse phases centered on the principle peak, the interpulse and pulse minimum are given for both luminosity states. There is no evidence for any of the cyclotron features seen from 4U0115-63. A feature may be evident at ~ 20 keV in the higher luminosity spectrum, although uncertainties in the background subtraction make its reality doubtful. The iron line is clearly seen in the pulse minimum spectrum.

## IV. PENCILS OR FANS?

The fundamental issue that remains unresolved for systems where the luminosity is too low for a radiative shock to form is whether or not a collisionless shock de-accelerates the infalling material. Basko and Sunyaev (1976a) have solved the one-dimensional hydro-dynamic and radiative diffusion equations (see also Wang and Frank 1981) and find that the outgoing radiation will not shock the inflowing gas stream until

$$L_x > 5 \times 10^{36} \cdot \frac{\sigma_T}{\sigma_s} \cdot r_5 \cdot R_6^{-1} \cdot M_{1.4} \text{ erg s}^{-1} \qquad (1)$$

where $r_5$ is the radius of the accretion funnel in units of $10^5$ cm, $R_6$ and $M_{1.4}$ are the radius and mass of the neutron star in units of $10^6$ cm and 1.4 $M_\odot$ respectively. Since an electron in a $> 10^{12}$ G magnetic field can only move

freely along the field lines the scattering cross-section for photons propagating out of the accretion column is dependent on energy, polarization and propagation angle relative to the field lines (Canuto, Lodenquai and Ruderman 1971; Lodenquai et al. 1974); hence $\sigma_s$ is the effective scattering cross section relative to the Thomson value $\sigma_T$. If the inflowing particles give up their kinetic energy via Coulomb interactions in the outer layers of the neutron star, then the emission region will be a thin slab with a temperature that decreases with increasing optical depth. The angular dependence of the electron scattering cross-sections of the ordinary mode photons means that as the angle $\theta$ from the magnetic axis decreases we view deeper into the atmosphere. Since the photon density increases asymptotically with optical depth up to some cutoff value, a pencil beam of emission is formed (Basko and Sunyaev 1975). If a collisionless shock occurs there will be a cylinder of emission above the neutron star (Langer and Rappaport 1982), and it is unclear in which direction the photons will escape. At energies close to the cyclotron resonance, because of the large opacities along the direction of the accretion flow, the photons may escape in a fan beam. At energies far below this the magnetically induced reduction in the opacities and angular dependence of this effect may allow a pencil beam of emission (Nagel 1981a).

One possible observational solution to this problem is to examine the properties of the systems where $L_X > 10^{37}$ erg $s^{-1}$ and it is most likely that a radiative shock has formed. The observed similarities among these systems then constitute a template representative of the properties of a shocked emission region which can be compared with those of the lower luminosity systems. The $180^0$ phase reversals from GX1+4 and 4U1626-67 can be accounted for if there are pencil and fan beams in different energy bands (Nagel 1981a;

Wang and Welter 1981). This requires that the maximum of the fan beam only pass through our line of sight once, which for a magnetic declination $\delta$ and inclination to the rotation axis i gives $\delta + i < 90^{o}$. The dramatic reduction in the c oss section along the magnetic axis for ordinary mode photons well below the cyclotron resonance favors a fan beam interpretation of the high energy pulse. For 4U1626-67 the pencil beam can only dominate between 2 and 10 keV. In this configuration the "notch" is then naturally interpreted as the passage of the magnetic axis through the line of sight. This is not caused by the attenuation of the beam by material in the column (as is seen in the phase locked white dwarf system 2A0311-227, White 1981; Patterson, Garcia and Hiltner 1981), rather it results from the $10^{12}$ G magnetic field neutralizing the cross sections along the accretion column such that photons are not emitted into that direction (Nagel 1981a). It is interesting to note that Nagel (1981a) has, for a cylinder of emission, already qualitatively reproduced the light curve of 4U1626-67.

The orbital period of 4U1626-67 is 41 min, which was discovered from optical photometry where the X-ray pulse is seen reprocessed on the companion star (Middleditch et al. 1981). This allows the unique opportunity to sample the pulse light curve in two different directions. The reprocessed pulse profile obtained by Middleditch et al. is triple peaked and bears no resemblance to any of the X-ray light curves in Figure 5. As noted above the fan beam can only pass through our line of sight once when $\delta + i < 90^{o}$. Middleditch et al. find that the time delay of the reprocessed pulse give an orbital inclination of $\sim 20^{o}$. The companion however views the X-ray source from the orbital plane and if the neutron star's rotation axis is close to the orbital axis the companion should see the fan beam twice per rotation and the pencil beam once per rotation. The intense gravitational field will bend a

fan beam around the neutron star by $20^{o}$-$25^{o}$, so that the angular spacing of the three pulses will be approximately equally spaced, in reasonable agreement with the observations.

The presence of $180^{o}$ phase reversals in the pulse profile with energy are not a universal feature of the $> 10^{37}$ erg $s^{-1}$ pulsars. Cen X-3 and SMC X-1 are notable exceptions with luminosities during our observations of $\gtrsim 10^{38}$ erg $s^{-1}$. The lack of any $180^{o}$ change in the hard pulse with energy might be a line of sight effect such that only one beam is visible to us. Also, the conditions at the polar cap may vary such that in these cases the relative strengths of the two beams are substantially different. The interpulse of Cen X-3 is only evident at low energies (Figure 12) and it is plausible that this is from a pencil beam similar to that seen from GX1+4 (Figure 1). It is plausible that in the $10^{37}$ to $10^{38}$ erg $s^{-1}$ regime we are observing a transition from pencil beam dominated emission to fan beams caused by the increasing height of the radiative shock above the pole (see also Wang and Welter 1981). The $180^{o}$ phase reversal seen from Her X-1 below ~ 1 keV (Figure 1) and the reduction in pulse amplitude at low energies in SMC X-1 can be explained in terms of reprocessing in the magnetosphere (e.g. McCray and Lamb 1976), however models that invoke a similar combination of pencil and fan beams also cannot be ruled out.

In the case of 4U0900-40 where $L_{x} \sim 10^{36}$ erg $s^{-1}$, the spectra indicate that the break up of the pulse at low energies is caused primarily by two regions of hardening centered at $\phi \sim 0.25$ and $\phi \sim 0.75$ (Figure 8). These are very similar to the "notches" evident in the low energy light curves of GX1+4 and 4U1626-67, which we identify as the passage of the magnetic axis through the line of sight, i.e. a pencil beam configuration. A fan beam might exhibit sharp features in the light curve by attenuation due to the neutron star body

itself (Wang and Welter 1981), or by cyclotron absorption from material away from the main inflow (Elsner and Lamb 1976). The former is unlikely in this case because to produce the double peaked high energy light curve of 4U0900-40 the maximum of the fan beam must pass through the line of sight twice on each rotation ($i + \delta > 90^0$), which then makes it impossible for the beam to be symmetrically eclipsed by the neutron star. Alternatively, Elsner and Lamb (1976) suggested that the magnetic field near the surface has multipole components so that all the accreted material need not fall on the surface at one pole. If the field strength is a factor 10-100 below that at the dipole then as the material in the field lines above the higher order poles passes through our line of sight cyclotron absorption could cause the observed breakup at low energies. Unfortunately, this model is not as well developed as the thin-slab calculations and it is not possible to make a detailed comparison with the observations. The similarity of the regions of spectral hardening from 4U0900-40 to those seen in the pulse profiles of GX1+4 and 4U1626-67 is very striking, and favors a pencil beam configuration. The thin slab models considered by Basko and Sunyaev (1975), Kanno (1980), Nagel (1981a), Meszaros and Bonazolla (1981) and Meszaros et al. (1982) specifically predict the appearance of these features at low energies for optical depths through the atmosphere less than a few. The presence of the additional feature D3 (at $\phi \sim 0.08$ Figure 7) and possibly at $\phi \sim 0.52$ suggests that the magnetic field on the neutron star may have a large quadrapole term.

It is likely that a similar explanation holds for the breakup of the low energy light curve of A0535+26 (Bradt et al. 1976). There is also a tendency for the light curves of 4U1223-62, 4U1538-52 and possibly OA01653-40 to fragment at lower energies (Figure 1).

## V. CYCLOTRON LINES

The restriction of the hard pulsed emission from Her X-1 to either a pencil or a fan beam would have important consequences for the modelling of the cyclotron feature. Calculations to date have suggested that for a pencil beam an absorption line at ~ 35 keV is more likely (Meszaros 1978; Yahel 1979; Bussard 1980; Wang and Frank 1981; Nagel 1981a,b). Any discussion of the direction of the beaming must account for all the properties of the Her X-1 pulse. If the intensely pulsed component below 1 keV results from the reprocessing of a hard pulse beamed from the neutron star then the models discussed to date by McCray and Lamb (1976), Basko and Sunyaev (1976a) and McCray et al. (1982) specifically require a pencil beam configuration to reproduce the phase reversal between the soft and hard pulsations. Additional observational evidence for a pencil beam is that the pulse of Her X-1 develops a notch below 20 keV close to pulse maximum (Figure 1; Voges et al. 1982; Pravdo et al. 1978) which is associated with a region of spectral hardening (Pravdo et al. 1977b). Pravdo et al. (1977b) suggested that this results from a direct minimally obscured view deep into the emission region, along the magnetic axis (see also Pravdo et al. 1978). The findings presented in the previous section support this hypothesis.

The change in the cyclotron feature of 4U0115+63 from absorption to emission at different pulse phases suggests that during the primary pulse when the line is in absorption, we are observing a continuum source transmitted through a magnetized plasma, while during the interpulse the background continuum is no longer dominant and the magnetized plasma itself is in emission i.e. the primary peak is a pencil beam and the interpulse is a fan beam leaking out the sides of the accretion column. The observational advantage of this source over Her X-1 is that because the magnetic field

strength is lower, these features appear at lower energies, in particular the continuum at energies higher than the feature is accessible. The similarity of the pulse peak spectrum of 4U0115+63 to that of Her X-1 in all but the energy of the high energy break strongly suggests that the pulse from Her X-1 is a pencil beam and that there is a cyclotron absorption feature at ~ 35 keV. There is also an interpulse in the Her X-1 pulse profile (Figure 1) which, by analogy with 4U0115+63, cautions us that there may be an emission feature in the off pulse Her X-1 spectrum that exagerates the depth of any absorption feature found in an on minus off pulse spectrum. It is notable that Voges et al. (1982) find evidence for an emission line in the off pulse spectrum at ~ 30 keV, although its statistical significance is low.

While the phase averaged spectrum of Cen X-3 and its pulse profile are similar to those of 4U0115+63, the pulse phase spectral properties are quite different; in particular there is no evidence for any cyclotron lines. This serves to emphasize that the appearance of cyclotron features is the exception rather than the rule. It may well be that there is some critical luminosity at which these features can be seen, and that at higher or lower values variations in a variety of parameters, such as the optical depth of the atmosphere or height of the shock, that may cause them to become either very small or smeared out. We note that the luminosity of Her X-1 is similar to that of 4U0115+63 (in outburst), and that this corresponds to the luminosity where a radiative shock might start to form.

There is a small dispersion in the sample between ~ 10 and 20 keV in the high energy cutoff energy, $E_C$, although above it much larger variations in the rate of decay, $E_F$, are seen. This steepening in the spectrum of X-ray pulsars has been interpreted by many as the result of the anisotropic energy dependence of the cross sections below the cyclotron resonance in $> 10^{12}$ G

magnetic fields (e.g. Boldt et al. 1976; Pravdo and Bussard 1980; Meszaros et al. 1982) and it may give an independent measure of the field strength. A cyclotron absorption line at ~ 35 keV in the spectrum of Her X-1 introduces a second factor that could contribute to the rate decay measured by our detectors (Bussard 1980), but as is well demonstrated by 4U0115+63 (cf. Figure 10) there must still be an intrinsic steepening with increasing energy in addition to any contribution from an absorption line. In the cases of Her X-1 and 4U0115+63 where the cyclotron lines are clearly seen and their energies $E_L$ can be directly compared with that of the break, there does indeed seem to be a similar ratio $E_L/E_C$ of ~ 1.5, which is encouraging. But we note that other parameters such as the temperature and optical depth of the neutron star atmosphere could also be important in determining the break energy, which is emphasized by the evidence for a change in the break energy of Cen X-3 associated with a change in luminosity (Figure 13).

## VI. THE SIZE OF THE HOT SPOT

The area on the surface of the neutron star over which the inflowing material impacts, generally known as the hot spot, is determined by the closest distance from the magnetic equator that material becomes threaded onto the field lines. For spherical accretion the material is probably stopped by a collisionless shock outside the magnetosphere and then penetrates its screening currents via the Rayleigh-Taylor instability. The material then falls in blobs (like rain) through the magnetosphere until various mechanisms allow it to become attached to the field lines (Arons and Lea 1976a,b; Elsner and Lamb 1976,1977). Arons and Lea (1980) suggest that the Kelvin-Helmholtz instability is probably the most efficient threading mechanism and that the resulting area of the hot spot is <u>inversely</u> proportional to the square root of $L_X$ i.e. the size of the hot spot decreases with increasing luminosity. When

$L_X < 10^{35}$ erg $s^{-1}$ a substantial fraction of the material may fall directly onto the surface without ever becoming attached to the field lines. If there is sufficient angular momentum for a Keplerian disk to form, it pinches the magnetosphere and penetrates via a transition zone where field lines thread the disk forcing material via the Kelvin-Helmholtz instability or magnetic flux reconection to become attached to the field lines (Ghosh and Lamb 1978,1979a). The agreement between accretion torque theory and the observed spin-up rates supports the hypothesis that the disk material does not penetrate far into the magnetosphere (Ghosh and Lamb 1979b). In this case the area of the hot spot is proportional to $L_X^{2/7}$ (Baan and Treves 1972), i.e. the area tends to increase with increasing luminosity. These two opposite trends in the hot spot area for the spherical and disk accretion should cause noticable differences in the properties of the two types of system, particularly for the low luminosity systems with $L_X < 10^{36}$ erg $s^{-1}$ that perhaps can be used to differentiate between disk and spherical accretion.

X Per, 4U1145-61 and 4U1258-61 all have $L_X < 10^{36}$ erg $s^{-1}$, with their low luminosities a consequence of the widely separated binary systems in which the neutron stars are found ($P_{orb}$ > 20 days cf. Rappaport and van den Heuvel 1981 and refs therein). 2S0114+63 and $\gamma$ Cas are other members of this class (Koenigsberge et al. 1983; White et al. 1982). In these cases the mass losing star is far from filling its Roche lobe and stellar wind capture drives the X-ray emission. The angular momentum carried by the accreted gas will force it to orbit the neutron star at a radius $r_d$. For an accretion disk to form this must be larger than the magnetospheric radius $r_m$. Following Shapiro and Lightman (1976)

$$\frac{r_d}{r_m} \sim 10^{-5} \cdot P_{10}^{-2} \cdot \left(\frac{M}{M_\odot}\right)^3 \cdot V_{1000}^{-8} \cdot \mu_{30}^{-4/7} \cdot L_{33}^{2/7} \cdot R_6^{2/7} \qquad (2)$$

where $P_{10}$ is the orbital period in units of 10 days, $V_{1000}$ the velocity of the wind as seen by the neutron star in units of 1000 km $s^{-1}$, $L_{33}$ the X-ray luminosity in units of $10^{33}$ erg $s^{-1}$, M is the mass of the neutron star and $R_6$ and $\mu_{30}$ are its radius and magnetic moment in units of $10^6$ cm and $10^{30}$ G $cm^3$. A disk can be present only if the condition $r_d/r_m > 1$ is satisfied, which requires an implausibly low wind velocity of $< 250$ km $s^{-1}$; the wind velocities in these systems are observed to be $\gtrsim 1000$ km $s^{-1}$ (Hammerschlag-Hensberge et al. 1980).

X Per, 4U1145-61 and 4U1258-61 probably represent the best approximations that we will find to spherically symmetric accretion in a binary system. As such they are particularly useful for testing the models of Arons and Lea and Elsner and Lamb, as well as for comparison with the more luminous systems where more localized hotspots on the neutron star are more likely. Figure 1 shows that the light curves of these pulsars not strongly pulsed, with both 4U1145-61 and 4U1258-61 showing a tendency for the modulations to become less pronounced at higher energies. It is clear from Figure 1 that these profiles are relatively featureless and energy independent when compared with those of the more luminous pulsars. Although this could be caused by coincidental alignments of $\delta$ and i that produce small modulations, or by low magnetic fields on the neutron star ($\sim 10^{11}$ G) reducing the magnetic beaming effects, it may, as noted by Wang and Welter (1981), lend support to the idea that in the spherically symmetric case the material does not become easily attached to the field lines.

If, as $L_x$ decreases, the area of the hot spot expands, then the modulation amplitude will decrease as the outer regions of the hot spot include lower field regions where the magnetic beaming effects are not the

same as at the poles. For $L_X < 10^{35}$ erg $s^{-1}$ the spot may cover the entire hemisphere. Indeed, this might be an attractive explanation for the lack of coherent pulsations from the related X Per-like systems $\gamma$ Cas and 2S0114+65 when $L_X \sim 10^{33}$ erg $s^{-1}$ (White et al. 1982; Koenigsberger et al. 1983). Alternatively, as noted by Elsner (1976) the onset of the Rayleigh-Taylor instability is a function of magnetic latitude and a large percentage of the material may enter the magnetosphere at low latitudes, forming a "hot band" around the neutron star. This may be responsible for the differences in the phase averaged spectra of X Per and 4U1258-61 relative to the higher luminosity systems discussed in §II. In these cases non-magnetic spectral calculations similar to those of Shapiro and Salpeter (1975) and Alme and Wilson (1973) may be more appropriate than the magnetically modified ones of Meszaros et al. (1982) and Langer and Rappaport (1982). The overall luminosity of the X-ray emission from X Per declined by a factor of 5 from 1 x $10^{34}$ erg $s^{-1}$ to 2 x $10^{33}$ erg $s^{-1}$ over a five year interval, with no obvious change in the structure of the light curve, or its modulation amplitude of ~ 40% peak to mean (cf. White et al. 1976, 1982). This suggests that at low luminosities the flow through the magnetosphere is relatively independent of the mass transfer rate.

The height of any collisionless shock above the pole will be greater than a stellar radius for $L_X < 10^{34}$ erg $s^{-1}$ (Langer and Rappaport 1982; Shapiro and Salpeter 1975). If there is a collisionless shock in these cases then we would expect that when the luminosity of the X-ray emission from X Per declined by a factor of 5, the corresponding increase in the shock height into lower field regions would have changed the pulse light curve (Langer and Rappaport 1982).

## VII. THE ORIGIN OF THE IRON EMISSION

One of the striking features of Figure 2 is the prominent iron emission between 6.4 and 6.7 keV detected from 11 out of our sample of 14 pulsars with EWs ranging from 100 to 600 eV. In most cases the width of the line is not resolved and we can only set a limit to its FWHM of $\lesssim$ 1.2 keV, comparable to the detector resolution. For GX1+4 a width of 2 ± 1 keV is observed (Table 1) and from Her X-1 there is evidence for double lined structure (Pravdo et al. 1977a). For easy intercomparison all of the values given in Table 1 assume a single gaussian line. Uncertainties in the detector callibration and sensitivity to the underlying continuum limit our best estimates of the line energies to an absolute error of ±5%. Most are consistent with energies between 6.4 and 7.0 keV. With a detector resolution at this energy of only ~ 17% more complex line profiles cannot be ruled out. There is no strong correlation between EW and $L_X$ (Figure 3). In Figures 5, 8 and 11 we show how the EW varies with pulse phase for GX1+4, 4U0900-40 and Cen X-3. Only for Cen X-3 is there evidence for variations in the EW with pulse phase, with a clear anti-correlation with intensity such that the line flux is approximately constant across the pulse. For GX1+4 and 4U0900-40 there is tantalizing evidence for variation at the limits of the 90% confidence error bars, but they are not conclusive because the line parameters are convolved with possible continuum variations across the pulse. During the observation of 4U0900-40 on Day 716 the EW was 510 ± 290 eV, compared to the 150 ± 40 eV seen on day 699 when the luminosity was a factor 3 brighter. Becker et al. (1979) also reported similar variations in the EW of the iron line of 4U0900-40, some of which may be related to the large changes in absorption caused by the stellar wind of the primary.

The iron line emission almost certainly does not come from within a few stellar radii of the neutron star surface. The plasma above the magnetic pole

cannot contribute because it will be fully ionized by the intense radiation field (Bai 1980b). Fluorescence of the neutron star surface is ruled out because the gravitational red shift of the line to ~ 5.5 keV is not observed. Because it subtends a small solid angle, the photosphere of the companion star can yield only a few tens of eV of fluorescent emission for cosmic abundances (Bai 1980a; Basko 1978; Hatchett and Weaver 1977), which should exhibit a strong orbital dependence in contrast to the orbital independence that is observed (Pravdo et al. 1977a). The solid angle subtended by the accretion disk could be larger than that of the companion star, but we still only obtain an EW of $\lesssim$ 75 eV using cosmic abundances, the fluorescent efficiency given by Bai (1980a), and a maximum disk semi-angle of $20^0$. If we assume that the metallicity of the companion stars are not all anomolously high, then this leaves two potential sites for the emission: the stellar wind of the primary, or the magnetosphere of the neutron star.

A. The Stellar Wind

In many of the OB supergiant/neutron star binaries large variations in absorption up to ~ $10^{23}$ H $cm^{-2}$ are seen, usually at preferred orbital phases. The three sources in Table 1 where this phenomenon has been well documented are 4U0900-40 (e.g. Kallman and White 1982; Becker et al. 1978), Cen X-3 (Schreier et al. 1976), and 4U1223-62 (Swank et al. 1976). While all the spectra given in Table 1 are taken from orbital phases where the absorption is at the minimum value seen from these systems, there must still be gas streams and asymmetries in the wind with optical depths $\gtrsim$ 0.1 to account for the phase related absorption. This material will add to the emission independent of its orientation to our line of sight to the neutron star, while it will act as an absorber only when it eclipses the X-ray source.

The EW of iron emission fluoresced in the wind can be estimated as

$$EW = \omega.\Delta\Omega.\int_{7.1}^{\infty} I(E) \cdot [1 - \exp(-\sigma(E) \cdot N_H)] \cdot dE/I(6.4)\ eV \quad (3)$$

where $\omega$ is the fluorescent yield (= 0.34 for cold material), $\Delta\Omega$ is the fractional solid angle, $\sigma(E)$ the cross section of iron taken from Fireman (1976), $N_H$ an equivalent column density of hydrogen assuming a cosmic abundance of iron of $4 \times 10^{-5}$ $N_H$ and I(E) the continuum spectrum. For the spectrum of 4U0900-40 and $\Delta\Omega$ = 0.5 we obtain for an $N_H$ of $10^{23}$ H $cm^{-2}$ an EW = 200 $\omega$ eV. There is evidence that the ionization structure of the wind in 4U0900-40 is anomolous (Kallman and White 1982). If there is a substantial optical depth of hydrogenic and helium like iron then $\omega$ = 1 since the Auger effect will be neutralized. Thus the asymmetries and gas streams in the winds of these OB supergiants may provide the means by which a significant fraction of the observed EWs and variations are produced. We cannot further pursue this discussion without a detailed estimate of the structure of the wind which goes beyond the scope of this paper.

B. The Magnetosphere

Many of the pulsars in Table 1 do not have companion stars with winds and gas streams capable of producing the observed iron lines. These include both the disk driven systems such as Her X-1 and the spherically symmetric stellar wind accretors such as 4U1258-61. The only other place where substantial material can build up to give sufficient optical depth for iron fluorescence is the magnetosphere. The discovery of an intense soft emission component from Her X-1 by Shulman et al. (1975), confirmed by Catura and Acton (1975), stimulated the idea that there may be optically thick material in the magnetosphere that absorbs and reprocesses the original emission from the hot spot. Pravdo et al. (1977a) and Basko (1980) discuss the possibility that the

iron emission seen from Her X-1 originates from this optically thick shell. Basko and Sunyaev (1976b) and McCray and Lamb (1976) proposed that this plasma layer is not optically thick over the magnetic poles and as the neutron star rotates it periodically shields the X-ray emitting hot spot, giving rise to the high energy pulse with a reprocessed soft pulse in anti-phase.

Following Basko and Sunyeav (1976a) we can estimate the optical depth $\tau$ through the magnetosphere to be

$$\tau \sim 0.15\ R_8^{-1/2} \cdot \eta^{-1} \cdot v_f^{-1} \cdot \frac{L_x}{L_{edd}} \cdot (1-\beta)^{-1}$$

where $R_8$ is the radius of the magnetosphere in units of $10^8$ cm, $\beta$ is the fraction of the accreting material not stopped until below the neutron star surface ( $\sim 0.4$, Basko and Sunyaev 1976a), $\eta$ is the fraction of the magnetosphere covered, and $v_f$ is the ratio of the velocity of the material to its free-fall value. Substantial fluorescent emission will be seen if $\tau > 0.1$ (Basko 1980). The EW would be proportional to $\eta\tau \propto v_f^{-1} L_x$.

From the EW results in Figure 3, it is clear that the EW is not proportional to $L_x$, as it would be if the $V_f$ range were negligable. As noted by McCray and Lamb (1976) $V_f$ is most likely to be small when the magnetosphere is close to the corotation radius and the corotating material can be held in the magnetosphere centrifugally (Elsner and Lamb 1976). The three sources where this might be occuring are Her X-1, SMC X-1 and 4U0115-63. However, the lack of any excessive EWs in these systems (Table 1, Figure 3) argues against there being any build up of material. Thus the data do not show clear correlations in agreement with the model.

The SSS spectra of Her X-1 and SMC X-1 do not show the phase dependent absorption features expected from an optically thick shell (McCray et al.

1982; Marshall, White and Becker 1983). This is also true of the spectra discussed in this paper. For the sources with the best counting statistics, such as GX1+4, we can set upper limits to an iron edge between 7 and 9 keV that imply $\tau_{Fe} < 10^{-2}$. This adds to the arguments that the pulse at energies greater than ~ 1 keV is not formed by screening of the hot spot by optically thick material in the magnetosphere. This does not necessarily mean that the iron emission cannot come from the magnetosphere. Optical depths of ~ 0.1 could still produce a fluorescent iron line with an EW of several hundred eV without any edge between 7 and 9 keV being detected by current instrumentation, especially if the gas is highly ionized (Basko 1980), or is located out of the direct line of sight.

McCray et al. (1982) proposed an scenario for the low energy pulse of Her X-1 where the high energy X-rays are intrinsically beamed and the reprocessing occurs exclusively on the inner edge of the disk. The inclination of Her X-1 is ~ $85^{o}$ (Rappaport and Joss 1982) so that the nearside of the disk is hidden from view and we see only the reprocessed radiation when the beam points away from us. McCray et al. (1982) note that the observed phase averaged iron EW of ~ 280 eV is a factor of 20 above that expected from simple fluorescence of the disk material. As outlined earlier, however, iron fluorescence can still come the magnetosphere (see also Pravdo et al. 1977a).

For spherical infall the optical depth for free falling material is given by

$$\tau \sim 0.02\, L_{36} \cdot R_6^{-1/2} \left(\frac{M}{M_o}\right)^{-1/2} \qquad (5)$$

and is substantially less than unity for $L_x < 10^{36}$ erg $s^{-1}$, in particular for 4U1258-61 and 4U1145-61. In these cases, too, material must accumulate in a

reservoir at the magnetosphere (cf. Arons and Lea 1976; Elsner and Lamb 1977). The fact that no iron emission with EW > 150 eV is seen from X Per (and $\gamma$ Cas) suggests that the optical depth of this material decreases at lower mass transfer rates. If the accumulated material covers the entire magnetosphere we should see an absorption edge between 7.1 and 9.1 keV. The upper limits to such an edge of $\tau_{Fe} < 0.4$ and $< 0.1$ for 4U1258-61 and 4U1145-61 respectively, are only just consistent with that expected and then only if the material is highly ionized, suggesting that again the material is out of the direct line of sight.

## VIII. SUMMARY AND DISCUSSION

In this paper we have illustrated how the observed properties of X-ray pulsars can help resolve some of the fundamental issues concerning the nature of accretion onto magnetized neutron stars. It is notable that a class of objects that extend over six orders of magnitude in luminosity shows little variation in the phase average spectra of its members. Figures 2 and 3 indicate a slight softening of the spectra with decreasing $L_X$, but there is certainly no dramatic change with $L_X$. The pulse profiles and pulse phase spectral variations, in contrast, exhibit considerable variety.

Some of the high $L_X$ pulsars display phase reversals between different energy bands and large variations in the high energy cutoff parameters as a function of pulse phase. In these systems we are probably observing both pencil and fan beams of emission, with the fan beam occuring at the highest energies where the opacity along the accretion column is greatest (Nagel 1981a). If collisionless (or radiative?) shocks are present in the lower $L_X$ systems we would expect to see properties similar to those of the high $L_X$ systems. All the lower $L_X$ systems maintain phase in different energy bands and have stable high energy cutoff parameters as a function of pulse phase.

The systems in the $10^{36}$-$10^{37}$ erg $s^{-1}$ band show the characteristic low energy break up of the pulse predicted by the optically thick thin slab models. This argues that in these cases there is Coulomb deceleration of the accretion flow in the outer atmosphere of the neutron star. The thin slab models appear to be applicable only in the $10^{36}$-$10^{37}$ erg $s^{-1}$ energy range because at higher luminosities radiative shocks become important and at lower luminosities the material falls over a very large area of the neutron star, not just the magnetic pole. When we consider the possible contributions to the pulse shape from material flowing through the magnetosphere we conclude that we cannot observe its effect for $L_X \lesssim L_{edd}$.

The orbital parameters and low luminosities of 4U1145-61, 4U1258-61 and X Per suggest that these sources are undergoing spherically symmetric accretion. The light curves of these sources seem to be much simpler and less energy dependent than those for $L_X > 10^{36}$ erg $s^{-1}$ which probably reflects the fact, as predicted by Arons and Lea (1976) and Elsner and Lamb (1976), that the material is distributed over a large part of the surface of the neutron star, away from the intense magnetic field at the pole. This probably is the reason that the X-ray spectra of X Per and 4U1258-61 do not exhibit below ~ 20 keV the hard power law characteristic of other higher $L_X$ systems.

The intense iron emission detected from many of these pulsars will provide an important diagnostic for the material outside and flowing through the magnetosphere. Proportional counters with an $E/\Delta E = 6$ at 6.7 keV can adequately detect these features, but they are not ideally suited for studying the structure of the line or its pulse phase variations. Further observational progress may have to await large collecting area detectors with $E/\Delta E > 30$ (e.g. Serlemitsos 1982).

Many pulsars show regions of spectral hardening or "notches" in the low

energy pulse. It is very likely that, as first suggested by Pravdo et al. (1977b), these are caused by the passage of the magnetic axis through our line of sight. Since the spectral hardening or "notch" is usually seen close to pulse maximum this again argues that in these cases we are observing pencil beams of emission.

The detection of electron cyclotron lines from 4U0115+63 at 11.5 keV and 23 keV gives new insight into the nature of the feature discovered in the spectrum of Her X-1 by Trumper et al. (1978). The two lines from 4U0115+63 are first seen in absorption during the pulse peak and then in emission during a broad interpulse ~ $180^{o}$ in phase later. This can be naturally interpreted in terms of a back-illuminated magnetized column, with the absorption lines at the pulse peak caused by the column passing in front of the hot spot and the emission lines seen when we view perpendicular to the field lines. Both Her X-1 and 4U0115+63 (in outburst) have similar luminosities that correspond to the point at which a radiative shock begins to appear above the pole. Any discussion concerning the direction of the beaming in Her X-1 must also account for the phase reversed low energy pulsations and the region of spectral hardening during the pulse peak. As discussed in §V these two points are more easily reconciled in terms of a pencil beam configuration. This together with the new results from 4U0115+63 presented here and theoretical arguments suggest that the feature in the on pulse spectrum of Her X-1 is an electron cyclotron line in absorption at ~ 35 keV.

## ACKNOWLEDGMENTS

Steve Pravdo, Bob Becker, Elihu Boldt, Peter Serlemitsos, Frank Marshall, and Richard Mushotzky made invaluable contributions to this study. We thank Peter Meszaros and Alice Harding for pointing out and discussing many of the outstanding problems. Some of the 4U0900-40 observations come from a

collaboration with Fred Lamb, Paul Boynton, John Deeter and Steve Pravdo and we thank them for letting us use the data here. Frank Shaffer is thanked for the preparation of the figures and Sandy Shrader for typing the manuscript.

## REFERENCES


Alme, M.L., and Wilson, J.R., 1973, Ap. J. 186, 1015.

Arons, J., and Lea, S.M., 1976a, Ap. J. 207, 914.

Arons, J., and Lea, S.M., 1976b, Ap. J. 210, 792.

Arons, J., and Lea, S.M., 1980, Ap. J. 235, 1016.

Bai, T., 1980a, Ap. J. 239, 328.

Bai, T., 1980b, Ap. J. 240, 264.

Baan, W.A., and Treves, A. 1973, Astr. Ap. 22, 421.

Basko, M.M., and Sunyaev, R.A., 1975, Astr. Ap. 42, 311.

Basko, M.M., and Sunyaev, R.A., 1976a, M.N.R.A.S. 175, 395.

Basko, M.M., and Sunyaev, R.A., 1976b, Soviet Astr. 20, 537.

Basko, M.M., 1978, Ap. J. 223, 268.

Basko, M.M., 1980, Astr. Ap. 87, 330.

Becker, R.H., Boldt, E.A., Holt, S.S., Pravdo, S.H., Rothschild, R.E., Serlemitsos, P.J., and Swank, J.H., 1976, Ap. J. 207, 167.

Becker, R.H., Boldt, E.A., Holt, S.S., Pravdo, S.H., Rothschild, R.E., Serlemitsos, P.J., Smith, B.W., and Swank, J.H., 1977a, Ap. J. 214, 879.

Becker, R.H., Swank, J.H., Boldt, E.A., Holt, S.S., Pravdo, S.H., Saba, J.R., and Serlemitsos, P.J., 1977b, Ap. J. 216, L11.

Becker, R.H., Rothschild, R.E., Holt, S.S., Pravdo, S.H., Serlemitsos, P.J., and Swank, J.H., 1978, Ap. J. 221, 912.

Becker, R.H., Boldt, E.A., Holt, S.S., Pravdo, S.H., Robinson-Saba, J., Serlemitsos, P.J., and Swank, J.H., 1979, Ap. J. 227, L21.

Boldt, E.A., Holt, S.S., Rothschild, R.E., and Serlemitsos, P.J., 1976, Astr. Ap. 50, 161.

Bonazzola, S., Heyvaerts, J., and Puget, J.L., 1979, Astr. Ap. 78, 53.

Bradt, H. et al., 1976, Ap. J. 204, L67.

Bussard, R.W., 1980, Ap. J. 237, 970.

Canuto, V., Lodenquai, J., and Ruderman, M., 1971, Phys. Rev. 10, 2303.

Catura, R.C., and Acton, L.W., 1975, Ap. J. 202, L5.

Davidson, K., and Ostriker, J.P., 1973, Ap. J. 179, 585.

Davison, P.J.N., 1977, M.N.R.A.S. 179, 35p.

Doty, J.P., Hoffman, J.A., and Lewin, W.H.G., 1981, Ap. J. 243, 257.

Elsner, R.F., 1976, Ph.D. dissertation, Univ. of Illinois.

Elsner, R.F., and Lamb, F.K., 1976, Nature 262, 356.

Elsner, R.F., and Lamb, F.K., 1977, Ap. J. 215, 897.

Fireman, E.L., 1974, Ap. J. 187, 57.

Ghosh, P., and Lamb, F.K., 1978, Ap. J. 222, L83.

Ghosh, P., and Lamb, F.K., 1979a, Ap. J. 232, 259.

Ghosh, P., and Lamb, F.K., 1979b, Ap. J. 232, 296.

Giacconi, R., Gursky, H., Kellogg, E., Schreier, E., and Tananbaum, H., 1971, Ap. J. 167, L67.

Hammerschlag-Hensberge, G. et al., 1980, Astr. Ap. 85, 119.

Hatchett, S., and Weaver, R., 1977, Ap. J. 215 285.

Holt, S.S., Boldt, E.A., Rothschild, R.E., and Serlemitsos, P.J., 1974, Ap. J. 190, L109.

Holt, S.S., and McCray, R., 1982, Ann. Rev. Astr. Ap. 20, in press.

Ives, J.C., Sanford, P.W., Bell-Burnell, S.J., 1975, Nature 254, 578.

Johnston, M., Bradt, H., Doxsey, R., Gursky, H., Schwartz, D., and Schwartz, J., 1978, Ap. J. 223, L71.

Kallman, T.R., and White, N.E., 1982, Ap. J. (Letters), in press.

Kanno, S., 1980, Pub. Astr. Soc. Japan 32, 105.

Kelley, R., Apparao, K., Doxsey, R., Jernigan, G., Naranan, S., and Rappaport,

S. 1981, Ap. J. 243, 251.

Kelley, R.L., Jernigan, J.G., Levine, A., Petro, L.D., and Rappaport, S., 1982, preprint.

Kirk, J.R., and Galloway, J.J., 1981, M.N.R.A.S. 195, 45.

Koenigsberger, G., Swank, J.H., Szymkowiak, A.E., and White, N.E., 1983, in preparation.

Koo, J-W.C., and Haymes, R.C., 1980, Ap. J. 239, L57.

Lamb, F.K., Pethick, C.J., and Pines, D., 1973, Ap. J. 184, 271.

Langer, S.H., McCray, R., and Baan, W.A., 1980, Ap. J. 238, 731.

Langer, S.H., and Rappaport, S., 1982, Ap. J. 257, 733.

Lodenquai, J., Canuto, V., Ruderman, M., and Tsuruta, S., 1974, Ap. J. 190, 141.

Lucke, R., Yentis, D., Freidman, H., Fritz, G., and Shulman, S. 1976, Ap. J. 206, 625.

Marshall, F.E., White, N.E., and Becker, R.H., 1983, Ap. J., submitted.

Mason, K.O., 1977, M.N.R.A.S. 178, 81.

Maurer, G.S., Johnson, W.N., Kurfess, J.D., and Strickman, M.S., 1982, Ap. J. 254, 271.

McClintock, J.E. et al., 1976, Ap. J. 206, L99.

McClintock, J.E., Rappaport, S., Nugent, J., and Li, F., 1977, Ap. J. 216, L15.

McCray, R., and Lamb, F.K., 1976, Ap. J. 204, L115.

McCray, R., Shull, J.M., Boynton, P.E., Deeter, J.E., Holt, S.S., and White, N.E., 1982, Ap. J., in press.

Meszaros, P., 1978, Astr. Ap. 63, L19.

Meszaros, P., and Bonazzola, S., 1981, Ap. J. 251, 695.

Meszaros, P., Harding, A.K., Kirk, J.G., and Galloway, D.J., 1982, preprint.

Middleditch, J., Mason, K.O., Nelson, J.E., and White, N.E., 1981, Ap. J. 244, 1001.

Nagel, W., 1981a, Ap. J. 251, 288.

Nagel, W., 1981b, Ap. J. 251, 278.

Parkes, G.E., Murdin, P.G., and Mason, K.O., 1980, M.N.R.A.S. 190, 537.

Parmar, A.N. et al , 1980, M.N.R.A.S. 193, 49p.

Patterson, J., Williams, G., and Hiltner, W.A., 1981, Ap. J. 245, 618.

Pravdo, S.H., Becker, R.H., Boldt, E.A., Holt, S.S., Serlemitsos, P.J., and Swank, J.H., 1977a, Ap. J. 215, L61.

Pravdo, S.H., Boldt, E.A., Holt, S.S., and Serlemitsos, P.J., 1977b, Ap. J. 216, L23.

Pravdo, S.H., Bussard, R.W., Becker, R.H., Boldt, E.A., Holt, S.S., and Serlemitsos, P.J., 1978, Ap. J. 225, 988.

Pravdo, S.H. et al., 1979, Ap. J. 231, 912.

Pravdo, S.H., and Bussard, R.W., 1981, Ap. J. 246, L115.

Rappaport, S., and Joss, P.C., 1977a, Nature 266, 123.

Rappaport, S., and Joss, P.C., 1977b, Nature 266, 683.

Rappaport, S., Markert, T., Li, F.K., Clark, G.W., Jernigan, J.G., and McClintock, J.E., 1977, Ap. J. 217, L29.

Rappaport, S., and van den Heuvel, E.P.J., 1981, IAU Symp. 98.

Rappaport, S., and Joss, P.C., 1982, preprint.

Rose, L.A. et al., 1979, Ap. J. 231, 919.

Rosenberg, F.D., Eyles, C.J., Skinner, G.K., and Willmore, A.P., 1975, Nature 256, 628.

Schreirer, E., Giacconi, R., Gursky, H., Kelley, E., and Tananbaum, H., 1972, Ap. J. 178, L71.

Serlemitsos, P.J., 1982, X-ray Astronomy in the 1980s: ed S.S. Holt, NASA TM

83848, 441.

Shapiro, S.L., and Lightman, A.P., 1976, Ap. J. 204, 555.

Shapiro, S.L., and Salpeter, E.E., 1975, Ap. J. 198, 671.

Shulman, S., Friedman, H., Fritz, G., Henry, R.C., and Yentis, D.J., 1975, Ap. J. 199, L101.

Skinner, G.K., Bedford, D.K., Elsner, R.F., Leahy, D., Weisskopf, M.C., and Grindlay, J., 1982, Nature 297, 568.

Staubert, R., Kendziorra, E., Pietsch, W., Reppin, C., Trumper, J., and Voges, W., 1980, Ap. J. 239, 1010.

Strickman, M.S., Johnson, W.N., and Kurfess, J.D., 1980, Ap. J. 240, L21.

Swank, J.H., Becker, R.H., Boldt, E.A., Holt, S.S., Pravdo, S.H., Rothschild, R.E., and Serlemitsos, P.J., 1976, Ap. J. 209, L57.

Tananbaum, H., Gursky, H., Kellogg, E.M., Levinson, R., Schreier, E., and Giacconi, R., 1972, Ap. J. 174, L143.

Trumper, J., Pietsch, W., Reppin, C., Voges, W., Staubert, R., and Kendziorra, E., 1978, Ap. J. 219, L105.

Voges, W., Pietsch, W., Reppin, C., Trumper, J , Kendziorra, E., and Staubert, R., 1982, Ap. J., in press.

Wang, Y.-M., and Frank, J., 1981, Astr. Ap. 93, 255.

Wang, Y.-M., and Welter, G.L., 1981, Astr. Ap. 102, 97.

Wheaton, Wm.A. et al., 1979, Nature 282, 240

White, N.E., Mason, K.O., Huckle, H.E., Charles, P.A., and Sanford, P.W., 1976a, Ap. J. 209, L119.

White, N.E., Mason, K.O., Sanford, P.W., and Murdin, P., 1976b, M.N.R.A.S. 176, 201.

White, N.E., Parkes, G.E., Sanford, P.W., Mason, K.O., and Murdin, P.G., 1978, Nature 274, 664.

White, N.E., and Pravdo, S.H., 1979, Ap. J. 233, L121.

White, N.E., Pravdo, S.H., Becker, R.H., Boldt, E.A., Holt, S.S., and Serlemitsos, P.J., 1980, Ap. J. 239, 655.

White, N.E., 1981, Ap. J. 244, L85.

White, N.E., Swank, J.H., Holt, S.S., Parmar, A.N., 1982, Ap. J., in press.

Worrall, D.M., Knight, F.K., Nolan, P.L., Rothschild, R.E., Levine, A.M., Primini, F.A., and Lewin, W.H.G., 1981, Ap. J. 247, L31.

Yahel, R.Z., 1979, Astr. Ap. 78, 136.

TABLE 1 - PHASE AVERAGED PROPERTIES

| SOURCE | PERIOD PULSE(S) | PERIOD ORBITAL(D) | $\alpha$ | $E_c$(keV) | $E_F$(keV) | EW(eV) | d(kpc) | log[$L_X$][k] |
|---|---|---|---|---|---|---|---|---|
| SMC X-1[j] | 0.71 | 3.9 | 0.5 | 17 ± 2 | 10 ± 3 | < 300 | 50 | 38.7 |
| HER X-1[c] | 1.24 | 1.7 | -0.05 | 20 | 7 ± 3 | 280 ± 30 | 5 | 37.4 |
| 4U0115+63 | 3.61 | 24 | -0.06 | ~ 8 | ~ 7 | 115 ± 50 | 3.5 | 37.0 |
| CEN X-3 | 4.84 | 2.1 | 0.16 | 11<br>8 | 8 | 228 ± 36 | 8 | 37.9<br>38.2 |
| 4U1626-67[b] | 7.68 | 0.03 | 0.4 | ~ 20 | ~ 6 | ? | ~ 6[d] | ~ 37.1 |
| LMC X-4[g] | 13.5 | 1.4 | -0.2 | 17 ± 2 | 22 ± 5 | < 100 | 55 | 38.8 |
| OA01653-40 | 38.2 | ? | 0.4 | 18 ± 3 | 26 ± 10 | 550 ± 100 | 1-5[e] | 35.4-36.8 |
| GX1+4 | 115 | ? | 0.0 | 10 ± 2 | 45 | 510 ± 80 | 9 | 38.0 |
| 4U1258-61 | 272 | > 20 | 1.1 | 20?[h] | ? | $570^{+430}_{-250}$ | 2 | 35.8 |
| 4U0900-40 | 283 | 9.0 | 0.13 | 20 ± 2 | 16 ± 2 | 510 ± 290<br>130 ± 50 | 1.4 | 35.9<br>36.4 |
| 4U1145-61 | 292 | > 20 | 0.40 | 16 ± 3 | 19 ± 10 | 620 ± 140 | 1.5 | 35.0 |
| 4U1538-52 | 529 | 3.7 | 0.42 | 17 ± 2 | 11 ± 3 | 572 ± 140 | 5.5 | 36.6 |
| 4U1223-62 | 695 | 41 | -0.07 | 19 ± 1 | 11 ± 2 | 255 ± 76 | 1.8 | 36.4 |
| 4U0352+30 | 835 | > 40 | ~1.2[a] | ---- | ---- | < 150 | 0.35 | 33.6 |

---

[a]Spectrum is best represented by a 12 keV thermal in the 2-20 keV band and a ~ 1.2 power law above 20 keV (White et al. 1982, Worrall et al. 1981)

[b]from Pravdo et al. (1979)

[c]from Pravdo et al. (1976,1978)

[d]deduced from the spin up rate given by Pravdo et al. (1979)

[e]deduced from the lack of any low energy absorption (Parmar et al. 1980)

[f]during the spectral measurement

[g]Pulsations only seen during flares (Kelley et al. 1982) - none were observed in the data reported here.

[h]from Maurer et al. (1982)

[j]from Marshall, White and Becker (1982)

[k]0.5-60 keV

TABLE 2 - 4U0115+63 LINE PARAMETERS

| | FUNDAMENTAL | 1ST OVERTONE |
|---|---|---|
| **EMISSION** | | |
| Energy (keV) | 11.75 ± 0.75 | 23 (Fixed) |
| FWHM (keV) | < 5 | 1 (Fixed) |
| Photons $cm^{-2}$ $s^{-1}$ | 0.10 ± 0.05 | $0.04^{+0.05}_{-0.04}$ |
| $\frac{\text{Line Luminosity}}{\text{Total Luminosity}}$ | (11 ± 5)% | (7 ± 7)% |
| **ABSORPTION** | | |
| Energy (keV) | 11.3 ± 0.9 | 23 (Fixed) |
| FWHM (keV) | < 5 | 1 (Fixed) |
| Photons $cm^{-2}$ $s^{-1}$ | 0.11 ± 0.07 | 0.05 ± 0.05 |

90% confidence errors

## FIGURE CAPTIONS

Figure 1 - The pulse light curves of 12 X-ray pulsars. Each is repeated for half a cycle for clarity. Given at the top right of each plot is the log of the luminosity in the 0.5 to 60 keV interval. The pulse period in seconds is shown at the top center. The data come from OSO-8 (Cen X-3, 4U1223-62); HEAO-1 A2 (4U0900-40, OA01653-40, GX1+4, 4U1626-67, 4U1538-52); Einstein SSS (SMC X-1, Her X-1) and the remainder mixture of HEAO-1 A2 (7-25 keV) and Einstein MPC (1-10 keV). In the latter case the observations were at different epochs and the light curves were aligned in the overlapping energy bands of the detectors.

Figure 2 - The phase-averaged incident spectra of 12 X-ray pulsars. The labels are the same as those in Figure 1. 4U1223-63 and Cen X-3 come from observations made by OSO-8, with the remainder from HEAO-1 A2. In the latter cases the solid points are from the MED and the open from the HED. The spectra were deconvolved using the best fit models in Table 1. Most of the iron lines are consistent with widths < 3 keV (see §II).

Figure 3 - The phase averaged spectral parameters verses $L_X$ for all the pulsars given in Table 1. The dashed lines illustrate the range of variation seen across the pulse. X Per and 4U1258-61 did not require any high energy cutoff. We note that high energy data from Maurer et al. indicate that the spectrum of 4U1258-61 may fall off very rapidly above ~ 20 keV. The upper value of $E_F$ of ~ 70 keV for GX1+4 is off scale.

Figure 4 - Left side: The pulse profile of GX1+4 in three energy bands as seen by HEAO-1 A2, note the 180° phase reversal from the lowest to the highest energy band. Right Side: The variation in $\alpha$, $E_F$ and the EW of the iron K line as a function of pulse phase. $E_C$ was fixed at 10 keV. The error bars are 90% confidence. The plots on both sides are repeated for half a cycle. The dashed lines represent the 2-7 keV (lower) and 25-60 keV (upper) light curves shown on the left.

Figure 5 - Left side - The pulse profile of 4U1626-67 as seen by HEAO-1 A2, taken from Pravdo et al. (1979). Right side - The variation in $\alpha$, $E_C$ and $E_F$ with pulse phase again taken from Pravdo et al. (1979). The dashed lines indicate the pulse profiles in the 3-14 keV (lower) and 14-30 keV (upper) energy bands shown on the left. The plots are repeated for half a cycle for clarity.

Figure 6 - The spectra at the indicated pulse phases (as defined by Figures 4 and 5) of GX1+4 and 4U1626-67. For clarity the spectra have been smoothed. These are a combination of Einstein SSS and HEAO-1 A2 spectra taken at different times.

Figure 7 - The pulse profile of 4U0900-40 seen by HEAO-1 A2 on three different occasions. The average count rate during each observation is shown at the top right of each plot. The absorption was, in each case, consistent with $\sim 10^{22}$ H cm$^{-2}$.

Figure 8 - The pulse light curve and variation of the spectral parameters with pulse phase of 4U0900-40 (cf. Figures 4 and 5).

Figure 9 - The HEAO-1 A2 spectra at three different pulse phases as indicated in Figure 8. The normalization of the pulse peak spectrum P in the lower plot has been increased by 30% to normalize the three spectra at ~ 20 keV.

Figure 10 - The incident spectra of the recurrent transient 4U0115+63 at three different pulse phases. These are indicated in the pulse profile shown for the 2-60 keV band. The three spectra are each offset from each other by one order of magnitude. The model used to deconvolve these spectra from the instrument response did not include any line features, so any apparent features could be sharper in the incident spectra.

Figure 11 - The ratios of the original PHA spectra used for Figure 10.

Figure 12 - The pulse profile and spectral parameters as a function of pulse phase for Cen X-3 as seen by OSO-8 when $L_X \sim 2 \times 10^{38}$ erg $s^{-1}$ (cf. Figures 4 and 5).

Figure 13 - The incident spectra of Cen X-3 at the three pulse phases indicated in Figure 12 for two different observations when the luminosity was different by a factor of 2 (the higher luminosity case is shown in Figures 2 and 12). There is some evidence that in the lower luminosity spectra the high energy break energy has increased to ~ 11 keV from ~ 8 keV.

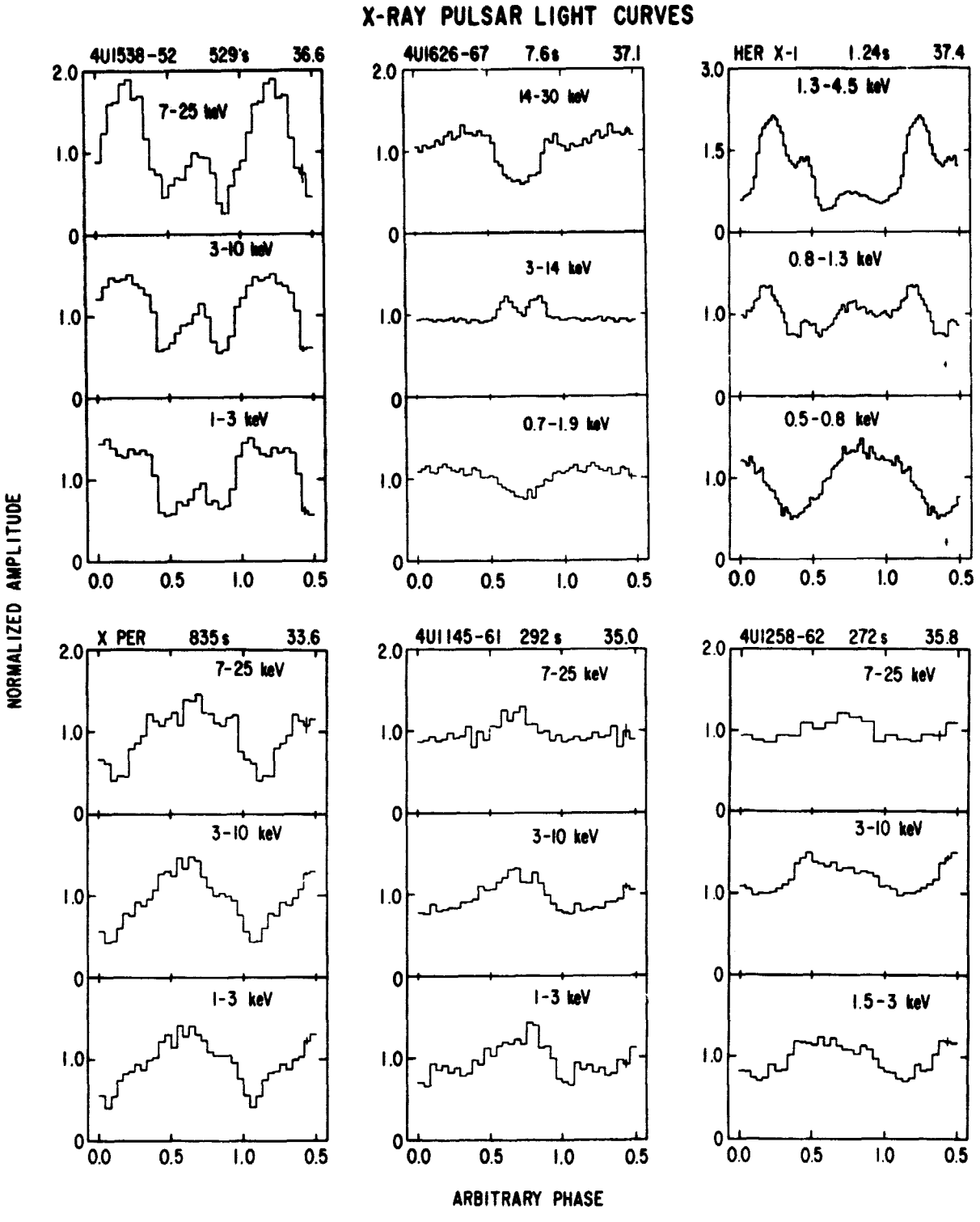


Figure 1 (left)

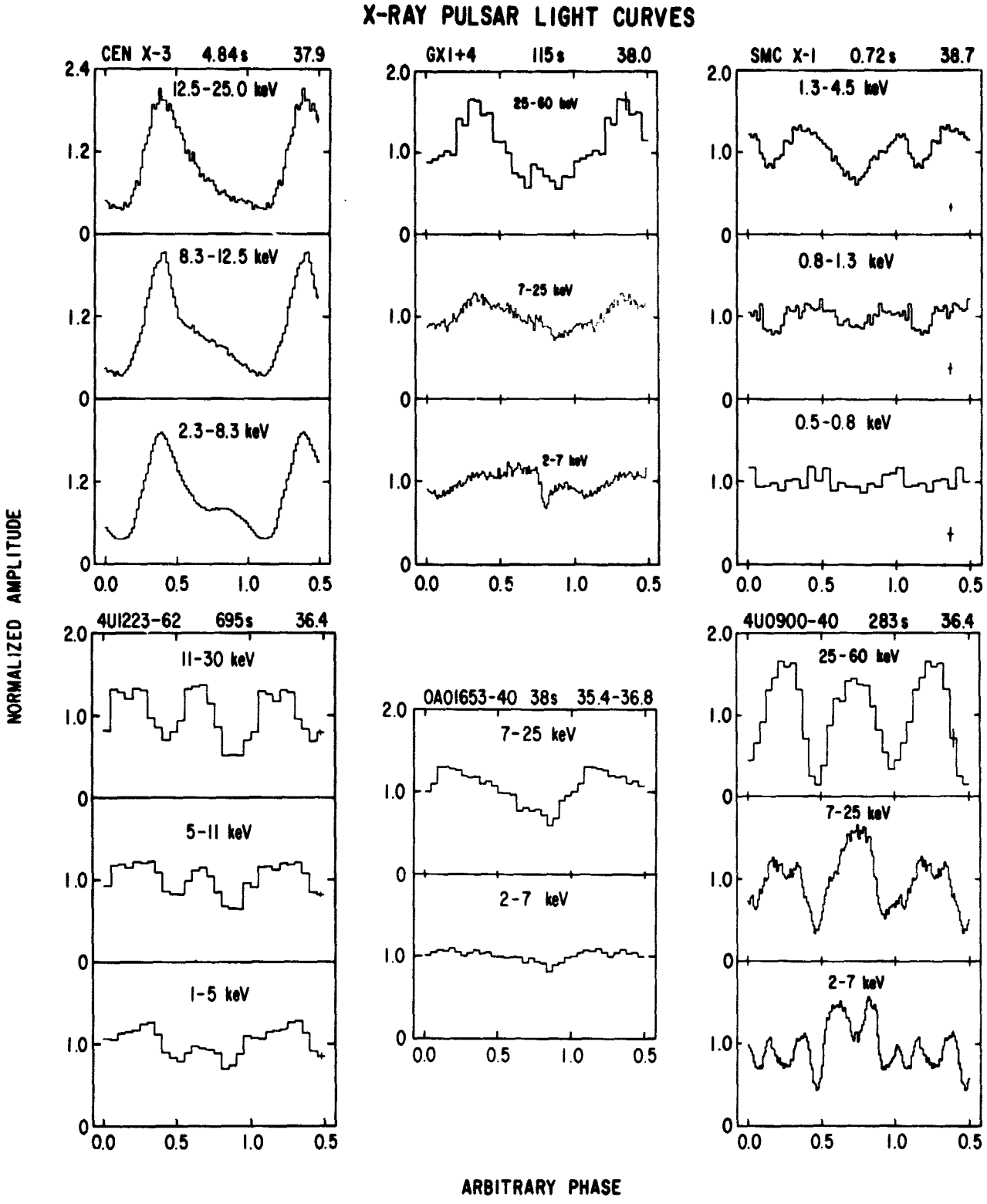


Figure 1 (right)

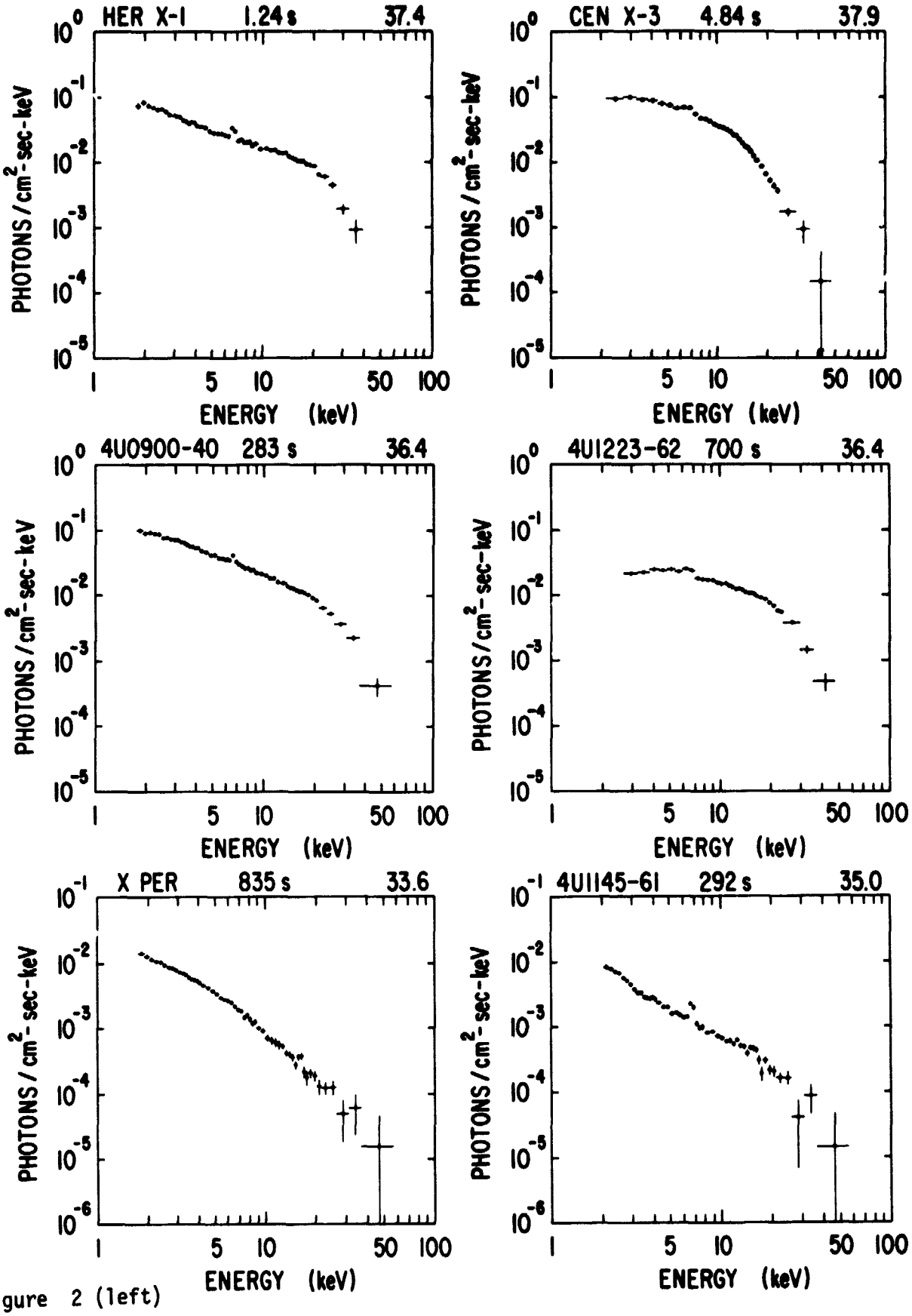


Figure 2 (left)

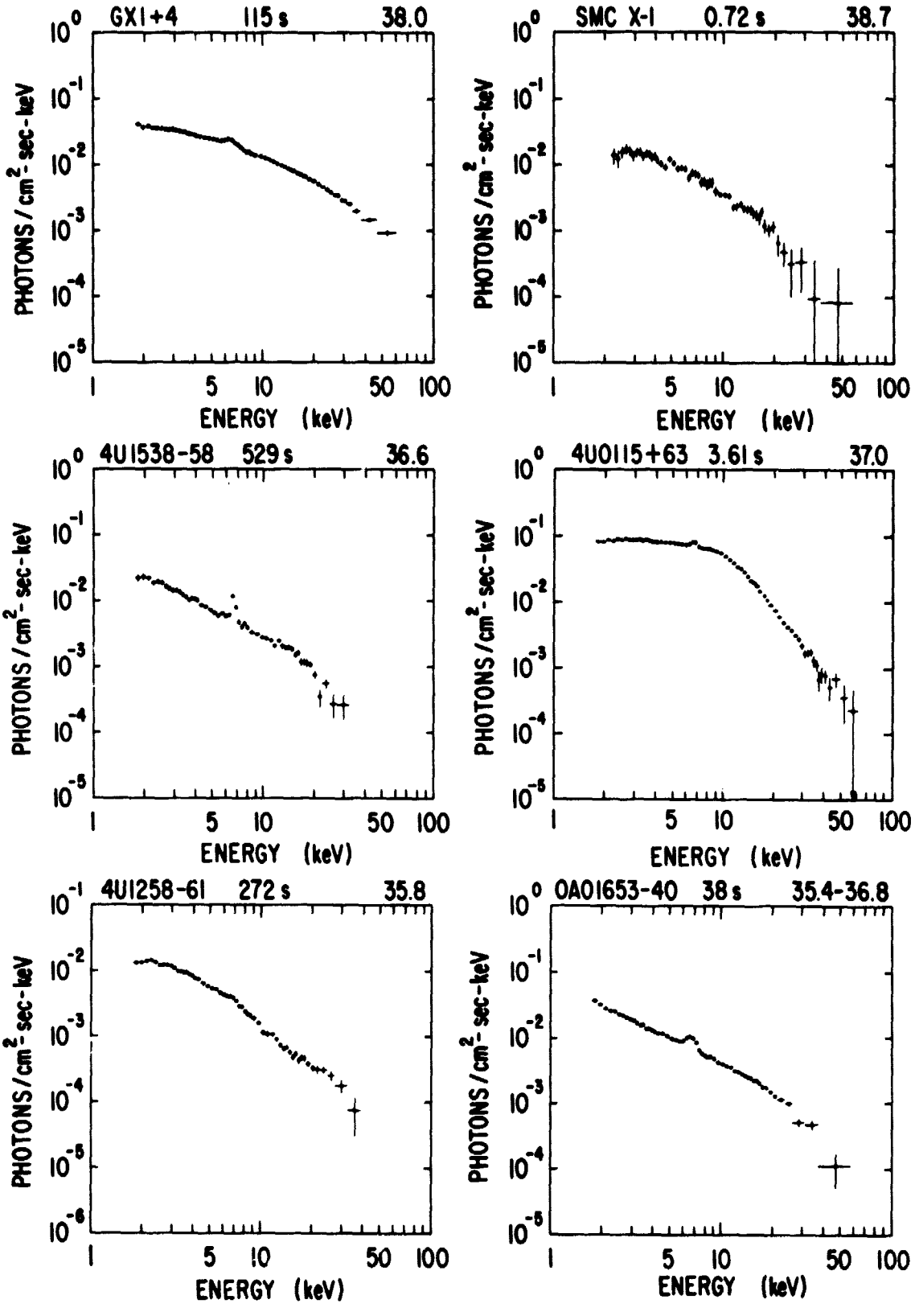


Figure 2 (right)

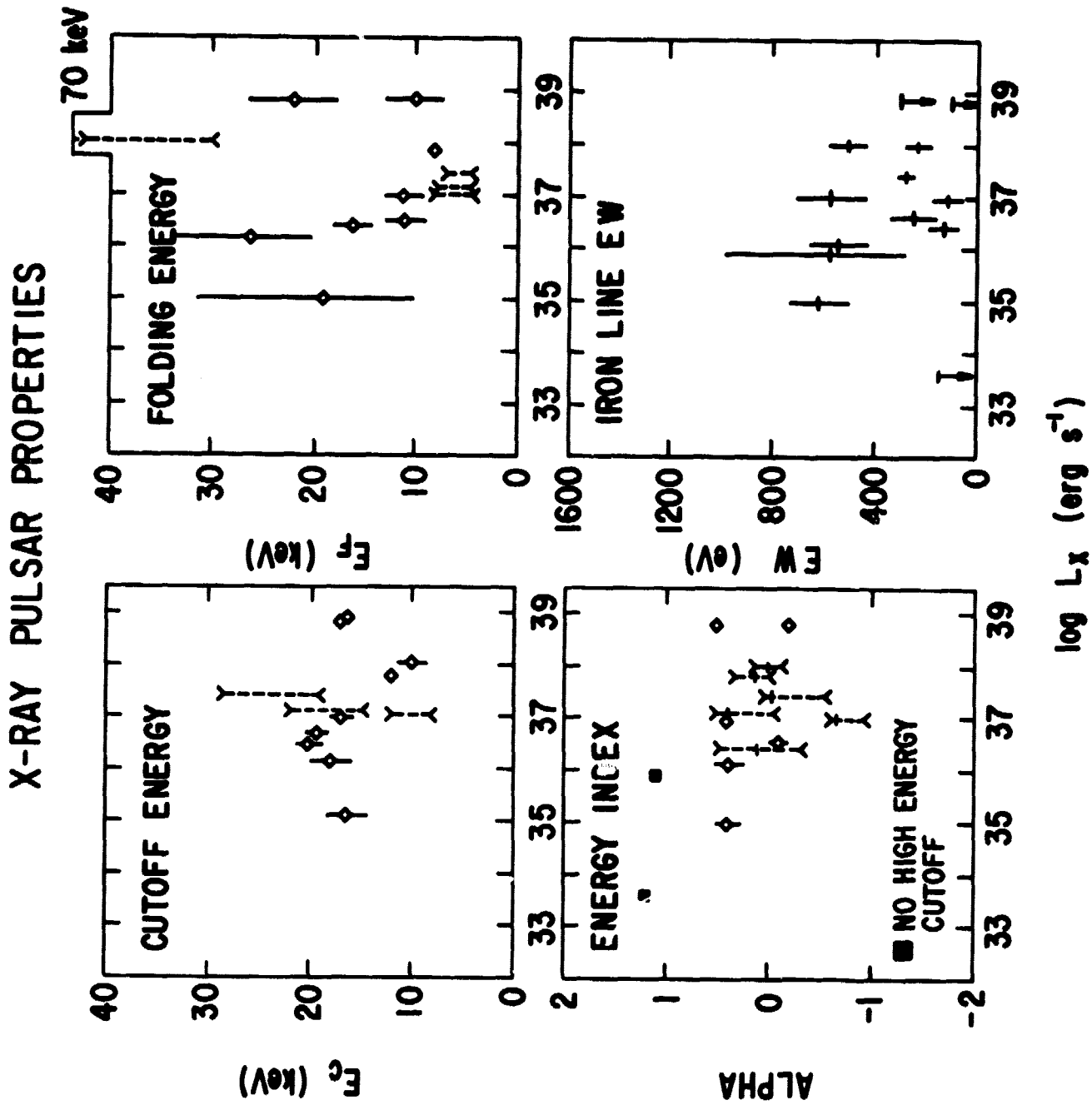


Figure 3

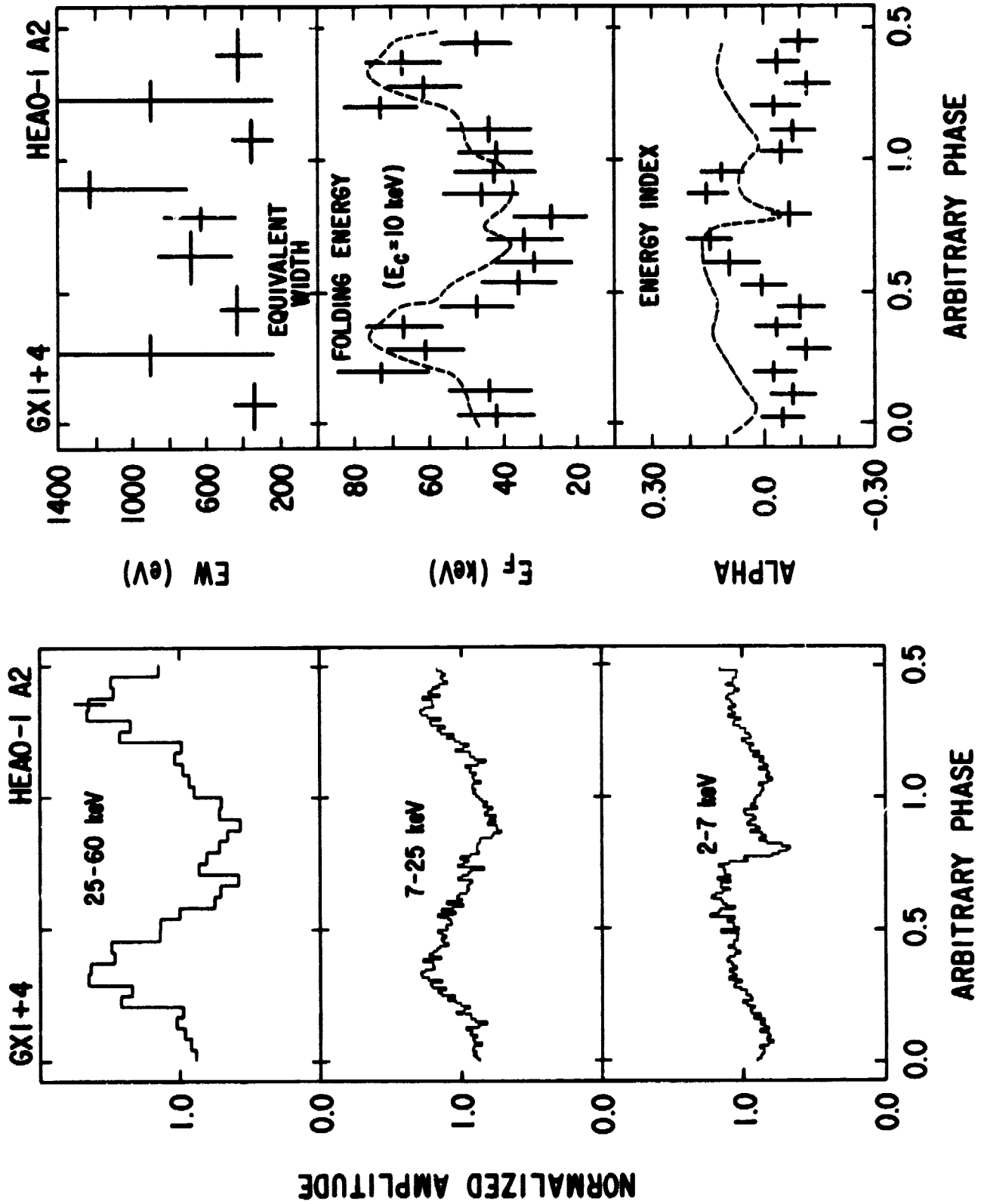


Figure 4

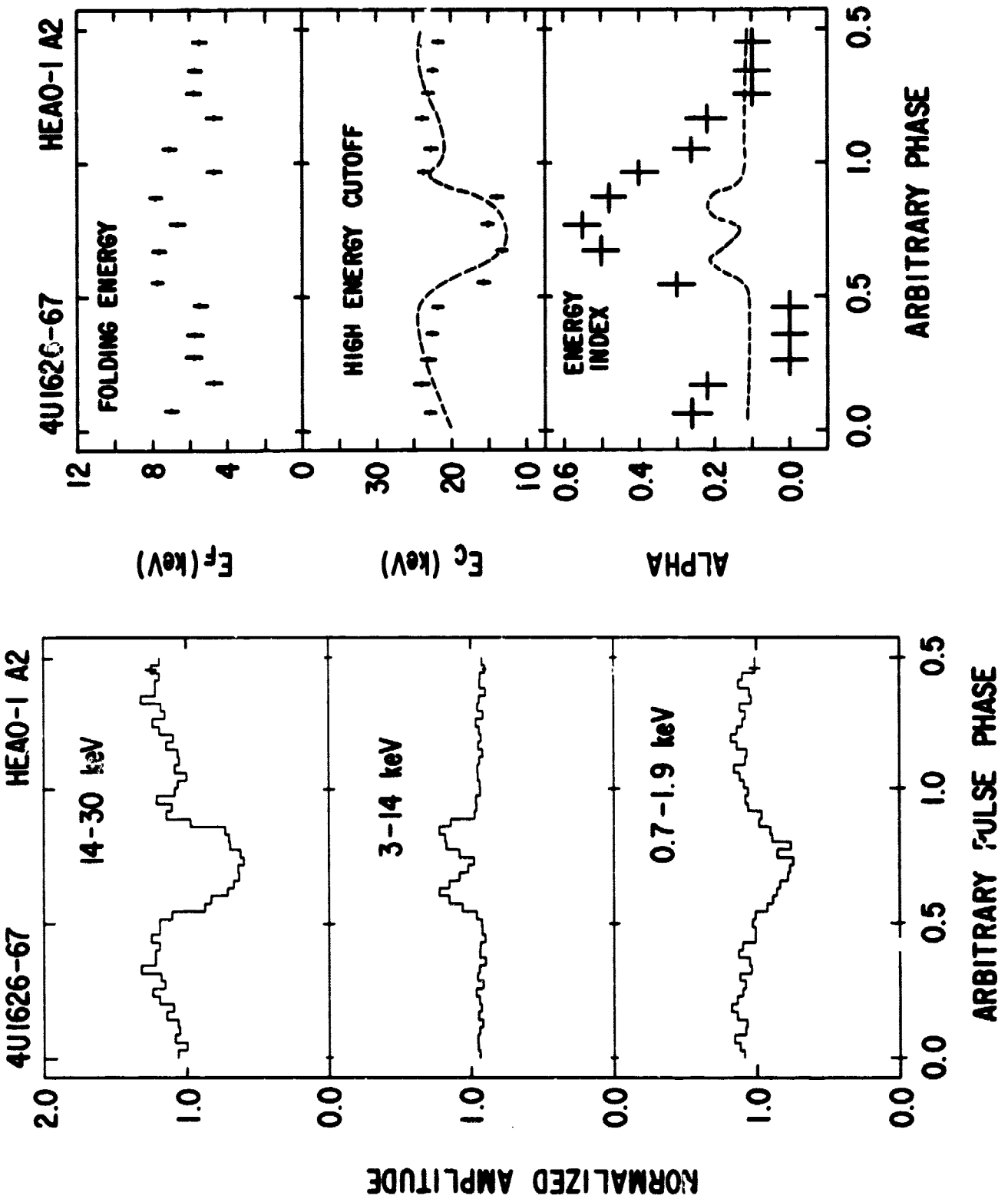


Figure 5

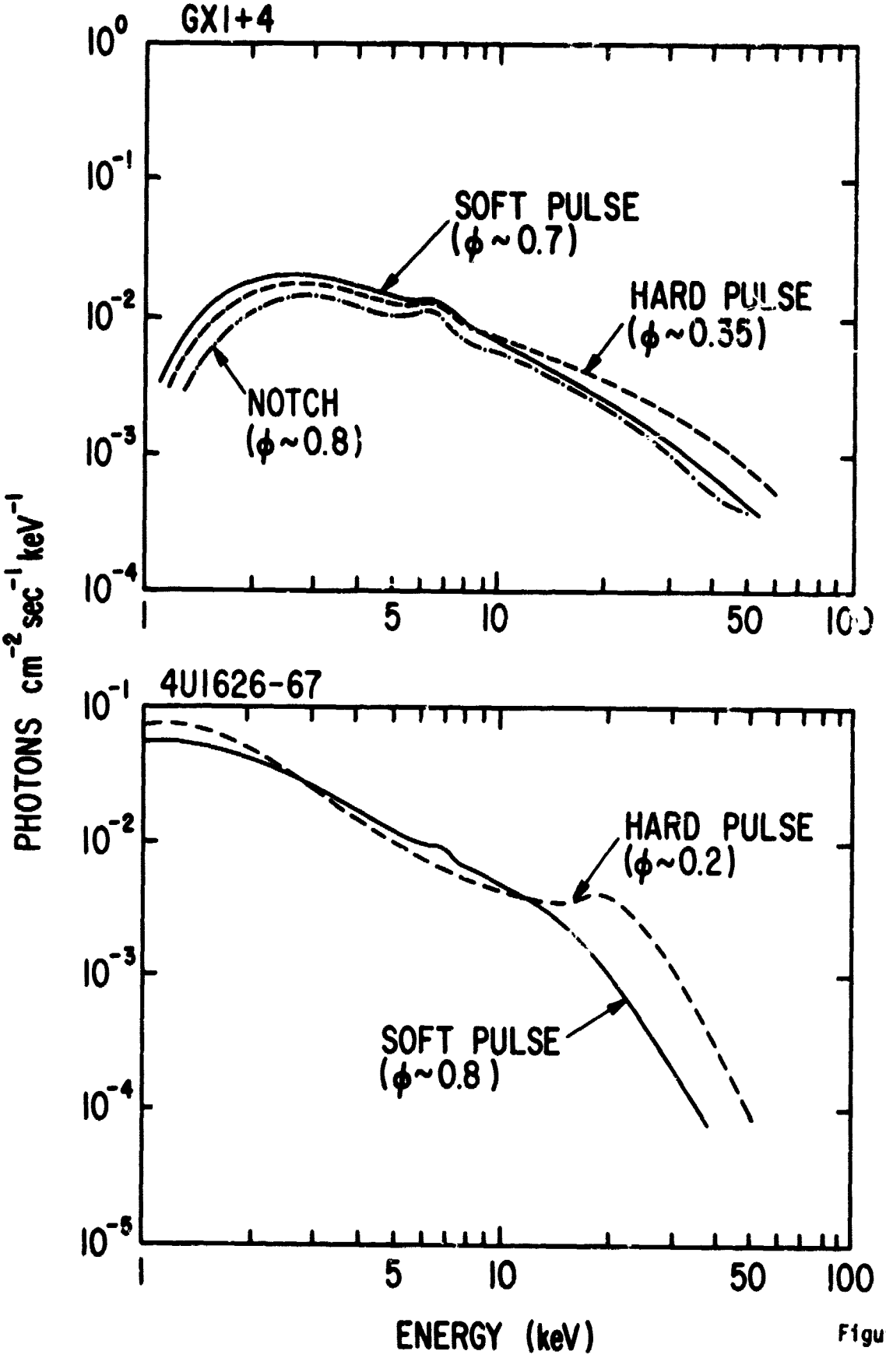


Figure 6

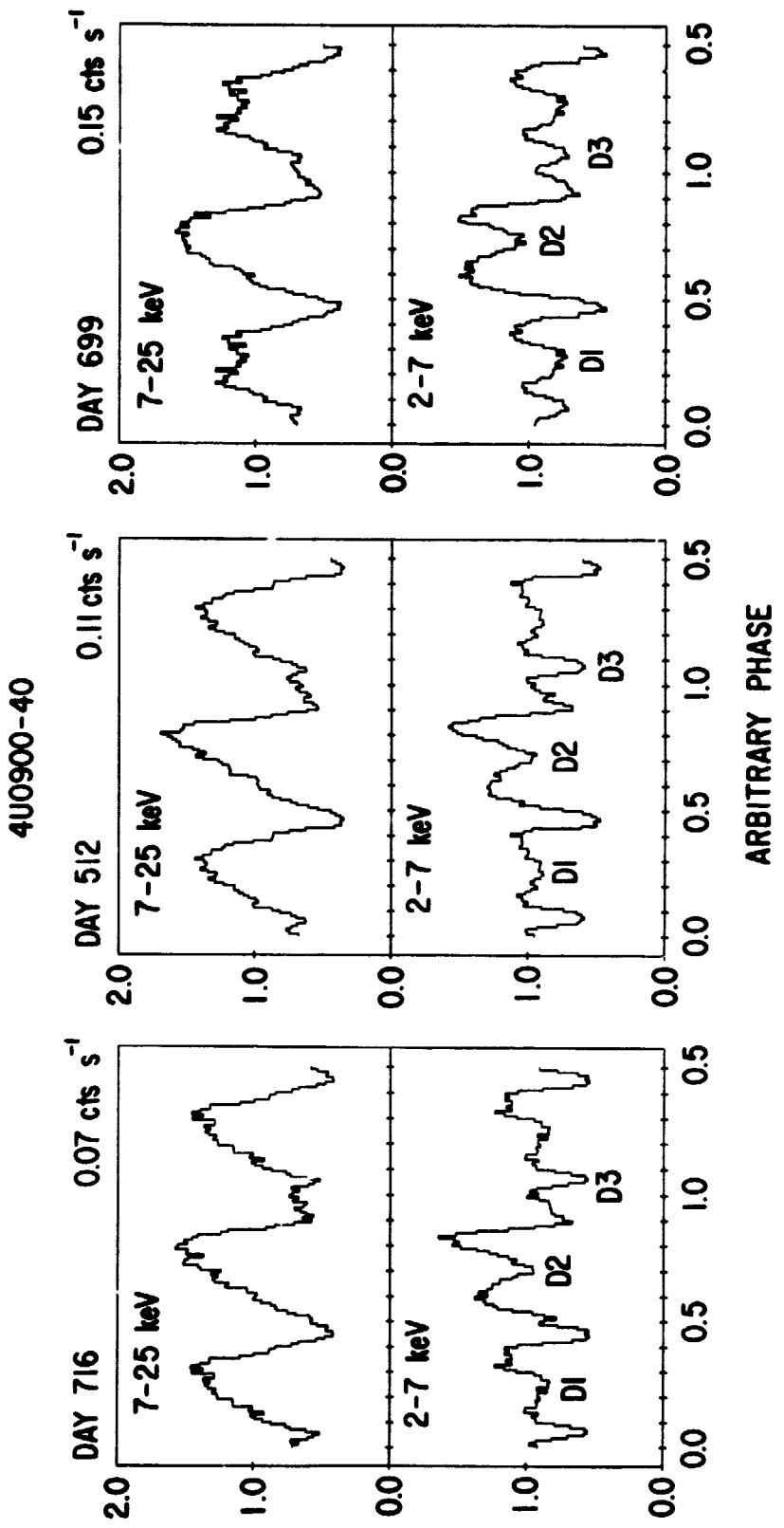


Figure 7

Figure 8

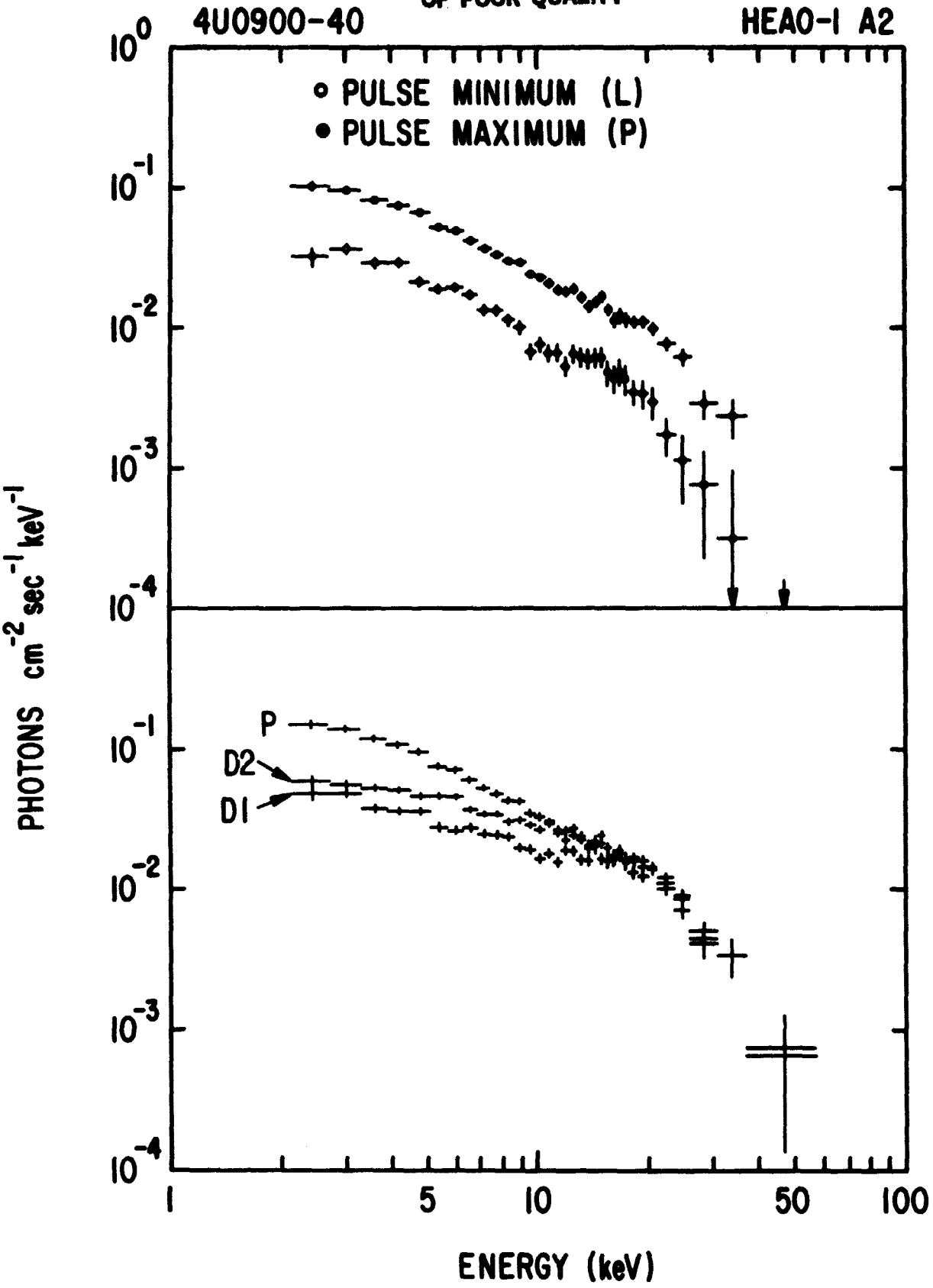


Figure 9

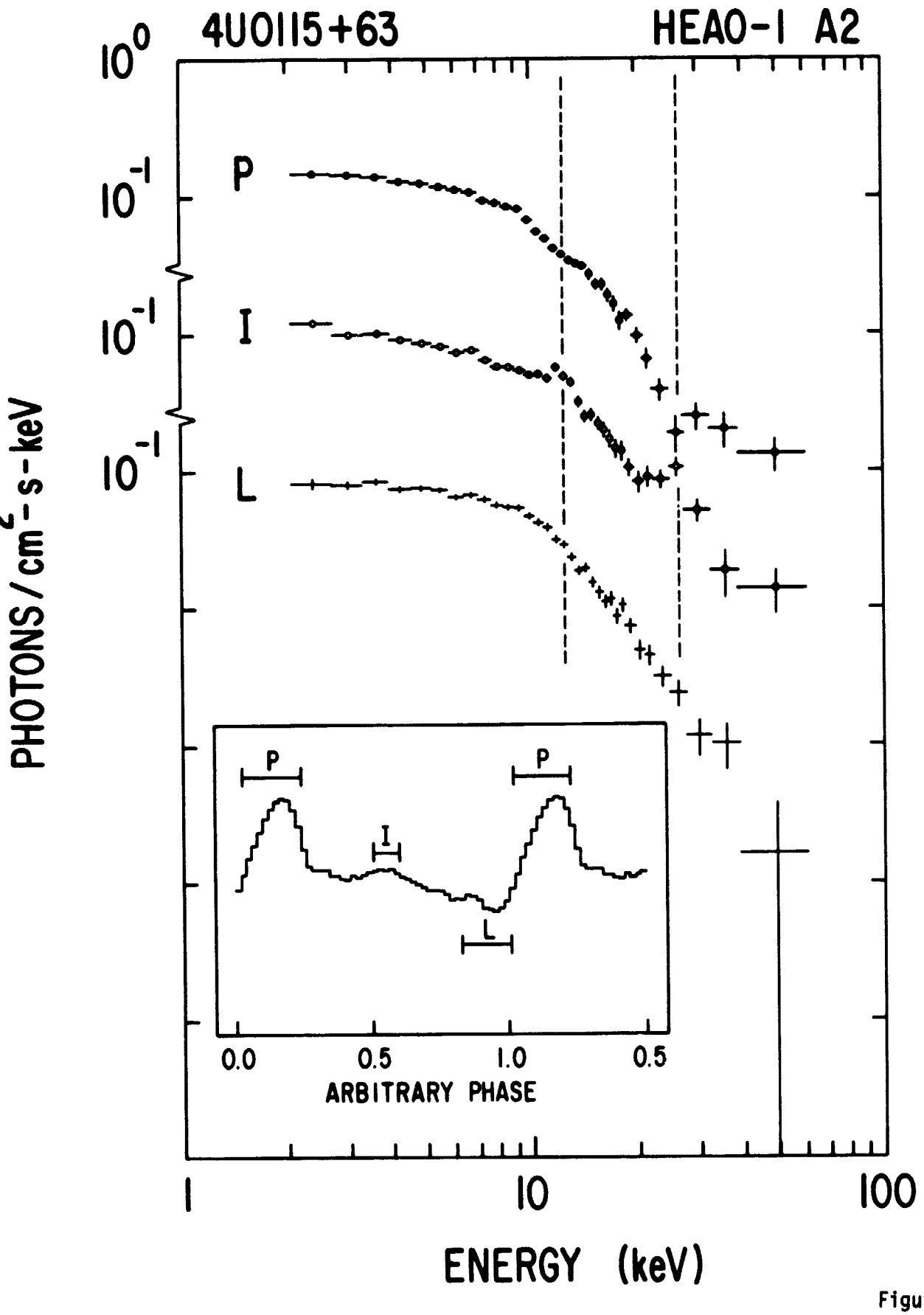


Figure 10

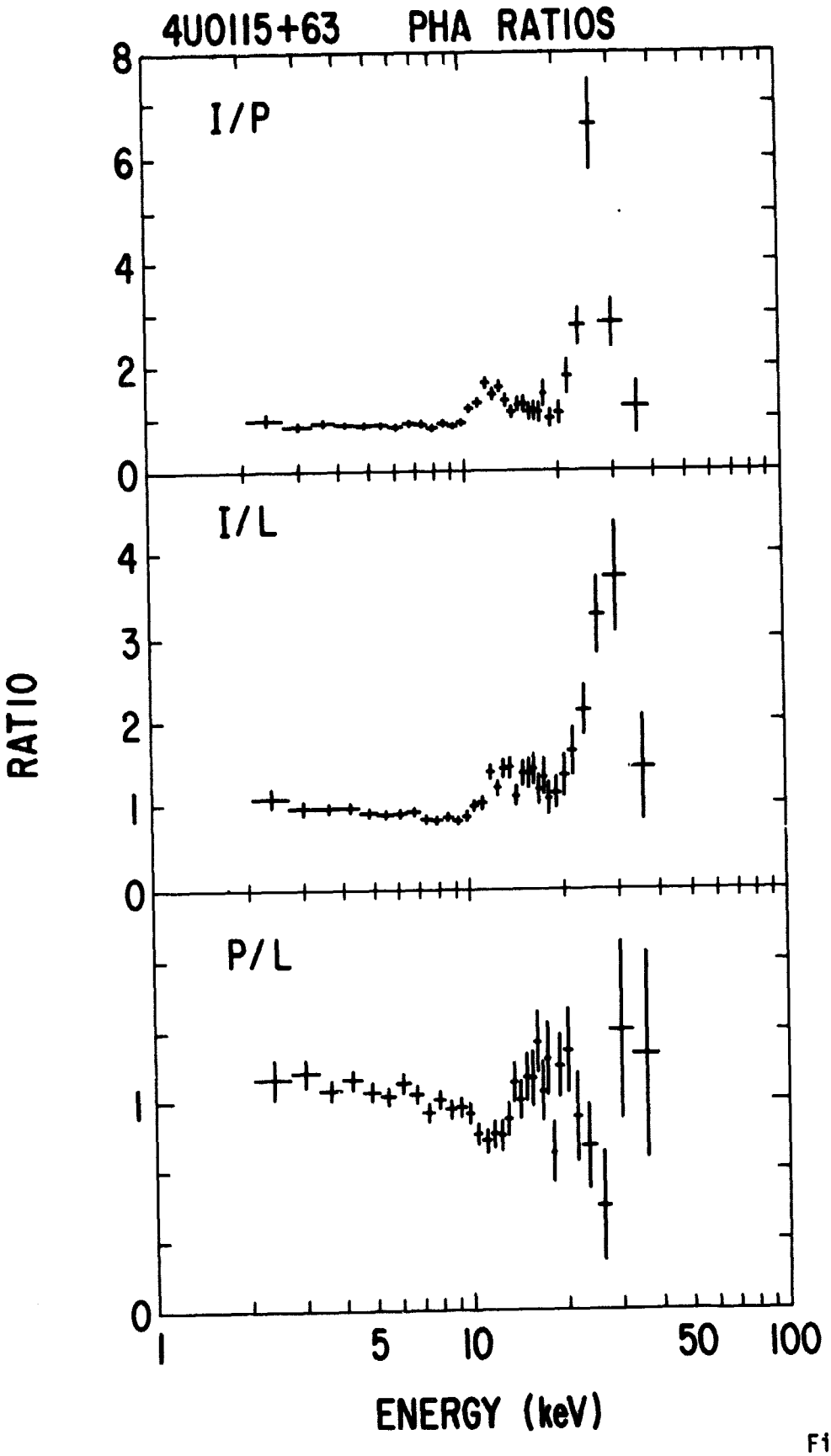


Figure 11

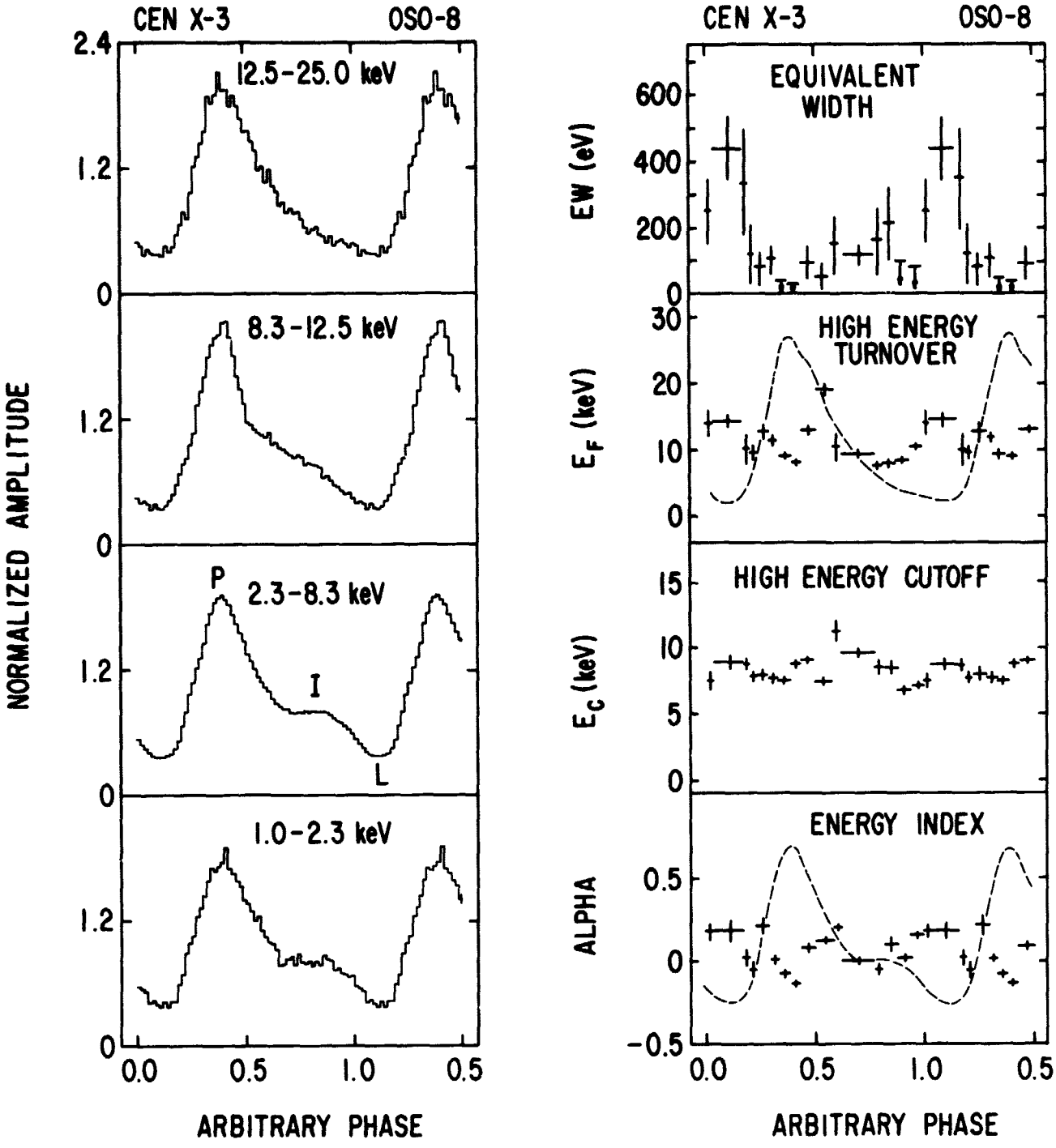


Figure 12

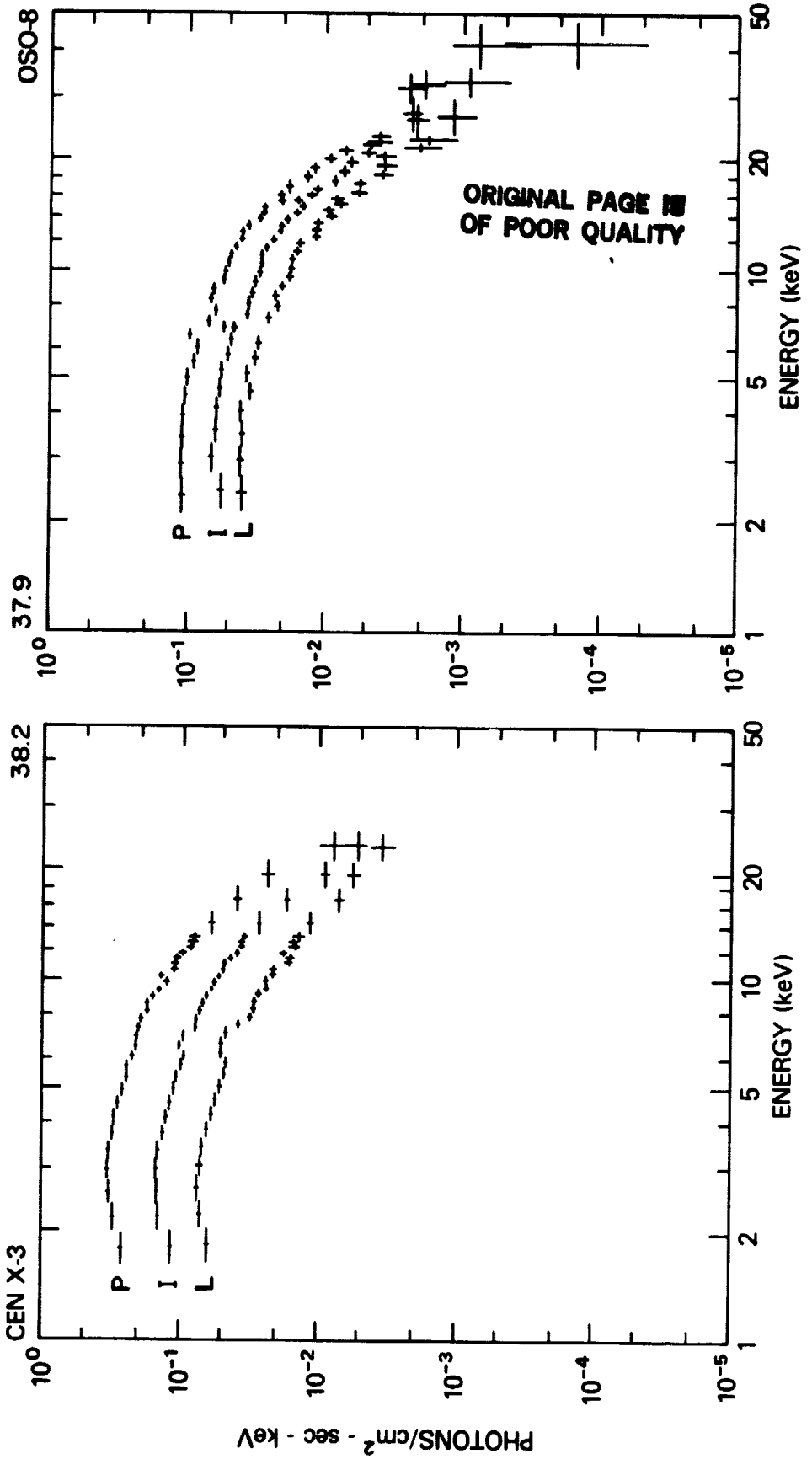
OSO-8
37.9
ORIGINAL PAGE IS
OF POOR QUALITY
P
I
L
ENERGY (keV)
CEN X-3
38.2
PHOTONS/cm² - sec - keV

Figure 13

ADDRESS OF AUTHORS

S.S. HOLT, J.H. SWANK, Code 661, Laboratory for High Energy Astrophysics, NASA/Goddard Space Flight Center, Greenbelt, MD 20771

N.E. WHITE, ESTEC, Postbus 299, 2200 A.G. Noordwijk Zh, The Netherlands